OPEN ACCESS

Original research

Human gut microbiota after bariatric surgery alters intestinal morphology and glucose absorption in mice independently of obesity

Fernando F Anhê ,[1] Soumaya Zlitni,[2] Song-Yang Zhang,[3] Béatrice So-Yun Choi ,[4] Cassandra Y Chen,[1] Kevin P Foley,[1] Nicole G Barra,[1] Michael G Surette,[5] Laurent Biertho,[4] Denis Richard,[4] André Tchernof ,[4,6] Tony K T Lam ,[3] Andre Marette ,[4] Jonathan Schertzer [1]

► Additional supplemental material is published online only. To view, please visit the journal online (http://dx.doi.org/10.1136/gutjnl-2022-328185).

For numbered affiliations see end of article.

Correspondence to
Dr Jonathan Schertzer, Department of Biochemistry and Biomedical Sciences, Hamilton, Hamilton, Canada; schertze@mcmaster.ca

Received 1 July 2022
Accepted 5 August 2022

To cite: Anhê FF, Zlitni S, Zhang S-Y, *et al*. *Gut* Epub ahead of print: [*please include* Day Month Year]. doi:10.1136/gutjnl-2022-328185

ABSTRACT

Objective Bariatric surgery is an effective treatment for type 2 diabetes (T2D) that changes gut microbial composition. We determined whether the gut microbiota in humans after restrictive or malabsorptive bariatric surgery was sufficient to lower blood glucose.

Design Women with obesity and T2D had biliopancreatic diversion with duodenal switch (BPD-DS) or laparoscopic sleeve gastrectomy (LSG). Faecal samples from the same patient before and after each surgery were used to colonise rodents, and determinants of blood glucose control were assessed.

Results Glucose tolerance was improved in germ-free mice orally colonised for 7 weeks with human microbiota after either BPD-DS or LSG, whereas food intake, fat mass, insulin resistance, secretion and clearance were unchanged. Mice colonised with microbiota post-BPD-DS had lower villus height/width and crypt depth in the distal jejunum and lower intestinal glucose absorption. Inhibition of sodium-glucose cotransporter (Sglt)1 abrogated microbiota-transmissible improvements in blood glucose control in mice. In specific pathogen-free (SPF) rats, intrajejunal colonisation for 4 weeks with microbiota post-BPD-DS was sufficient to improve blood glucose control, which was negated after intrajejunal Sglt-1 inhibition. Higher *Parabacteroides* and lower *Blautia* coincided with improvements in blood glucose control after colonisation with human bacteria post-BPD-DS and LSG.

Conclusion Exposure of rodents to human gut microbiota after restrictive or malabsorptive bariatric surgery improves glycaemic control. The gut microbiota after bariatric surgery is a standalone factor that alters upper gut intestinal morphology and lowers Sglt1-mediated intestinal glucose absorption, which improves blood glucose control independently from changes in obesity, insulin or insulin resistance.

WHAT IS ALREADY KNOWN ON THIS TOPIC?

⇒ Bariatric surgery is the most effective long-term treatment for type 2 diabetes (T2D).
⇒ Bariatric surgery lowers blood glucose before weight loss.
⇒ Blood glucose lowering is greater after malabsorptive compared with restrictive bariatric surgery.
⇒ Bariatric surgery changes the composition of the gut microbiota.
⇒ Gut microbiota can influence obesity and blood glucose.
⇒ It was not known if altered gut microbiota after bariatric surgery in humans is a standalone factor that lowers blood glucose.

INTRODUCTION

Obesity predicts the progression to type 2 diabetes (T2D), which is characterised by elevated blood glucose, glucose intolerance and insulin resistance.[1 2] Bariatric surgery promotes durable weight loss and is more effective than conventional medical interventions for long-term control of T2D.[3] Higher blood glucose is an independent risk factor for all-cause mortality, and bariatric surgery can increase survival in individuals with obesity.[4 5] Bariatric surgery rapidly lowers blood glucose and insulin resistance before any measurable weight loss.[6 7] However, it is still unclear how bariatric surgery promotes rapid versus durable blood glucose lowering facilitating T2D remission.

Laparoscopic sleeve gastrectomy (LSG) and biliopancreatic diversion with duodenal Switch (BPD-DS) span the spectrum of bariatric surgeries. LSG is a restrictive surgery that reduces the size of the stomach. BPD-DS is a malabsorptive and restrictive surgery because it creates a stomach pouch in addition to a long by-pass of the small intestine.[7] Compared with LSG, BPD-DS produces a more robust and sustained lowering of blood glucose, including greater T2D remission, which comes at the cost of more frequent side effects.[7 8]

Bariatric surgeries alter the composition and function of the intestinal microbiota.[6 7] Conserved shifts in gut microbiota after gastric bypass surgery in humans can promote weight loss and fat loss when transferred to germ-free mice.[9] There is evidence for a causal role for gut microbes in lowering fat mass after bariatric surgery in some preclinical models.[9–11] It is known that gut microbes influence host metabolism and can contribute to features of

WHAT THIS STUDY ADDS?

⇒ Microorganisms from humans after malabsorptive and restrictive bariatric surgery are sufficient to improve blood glucose control in mice.
⇒ Microbiota -mediated transmission of lower blood glucose required long-term (7 weeks) colonisation of germ-free mice by oral gavage and SPF rats (4 weeks) by intraluminal delivery.
⇒ Microbiota -mediated transmission of improved glucose control does not require changes in fat mass, insulin resistance, secretion, or clearance.
⇒ Microbiota lowering of blood glucose was due to lower sodium-dependent intestinal glucose absorption.
⇒ A subset of bacteria after bariatric surgery coincided with altered gut morphology and lower intestinal glucose absorption in mice.

HOW THIS STUDY MIGHT AFFECT RESEARCH, PRACTICE OR POLICY?

⇒ Microbiota in humans after bariatric surgery is sufficient to lower intestinal glucose absorption and blood glucose.
⇒ Development of probiotics or postbiotics that mimic the microbial effect of bariatric surgery and lower intestinal glucose absorption may promote durable blood glucose -lowering benefits in T2D without the drawbacks of bariatric surgery.

the metabolic syndrome beyond obesity, including insulin resistance and glycaemic control.[12 13] There is a dearth of information on a causal role for gut microorganisms after bariatric surgery as a standalone factor lowering blood glucose.[6 14]

Here, we colonised mice and rats with the faecal microbiota from the same patients before and after LSG or BPD-DS to test the causal relationship between gut microorganisms and blood glucose lowering by bariatric surgery and define the mechanisms of blood glucose lowering by the gut microbiota.

MATERIALS AND METHODS

Animals

Female C57BL6/N mice aged 16−24 weeks were originally sourced from Taconic and bred in the Central Animal Facility (CAF), McMaster University, under specific pathogen-free (SPF) or germ-free (GF) conditions. Mice received diet (Teklad global 18% protein rodent diet, Envigo, Cat# 2918) and water ad libitum. Female Sprague-Dawley rats aged 10 weeks (Charles River Laboratories) were housed in individual cages in a SPF room under a standard 12 hours light-dark cycle with ad libitum access to drinking water and chow (Teklad Diet 7012, Harlan Laboratories, Madison, Wisconsin, USA).

Bariatric surgery

Patients were enrolled in the Bariatric Surgery Care Centre of the Québec Heart and Lung Institute according to institutionally approved procedures. A detailed description of bariatric surgical procedures is in the online supplemental material.

Patient and public involvement

Many participants have been invited to attend a presentation held by clinicians and researchers in the context of the patient support group meetings. Two participants have shared their experience in videos.

Donor patients and faecal slurries

We selected three female patients with typical changes in body mass and glycaemic characteristics 12 months postsurgery (table 1). Stool samples, from the same patient were collected before and 12 months after BPD-DS or LSG, frozen immediately at −20°C and subsequently stored at −80°C. Faeces were later thawed on ice, resuspended in phosphate-buffered saline (1:10 (w:v)), aliquoted in 1.5 mL tubes and stored at −80°C until use. None of these patients took antibiotics at least 1 month before each faecal collection. Medication use and caloric intake are indicated in online supplemental tables 1 and 2.

Human-to-mouse faecal transplants

GF mice were exported from the axenic facility to the SPF room in closed sterile containers, which were opened under a disinfected biosafety cabinet (BSC). Freshly thawed faecal slurries from donor patients were orally gavaged into randomly assigned SPF (200 µL/mouse/3 times a week) and GF (200 µL/mouse/2 times a week) mice for a total of 9 weeks. Faecal slurries from one donor patient were used to colonise two to five mice, and separate mice were used for testing the faeces from the same patient before and after surgery. After the initial colonisation, GF mice were transferred (single-housed) to sterile cages with access to sterile water, which were refreshed weekly. SPF mice were kept four mice per cage with water and cage refreshed weekly. Handling of colonised GF mice was performed under a BSC. All mice were kept in ventilated cages in positive pressure mode.

Intestinal glucose absorption

In vivo intestinal glucose absorption was measured after 6 hours fasting in GF mice colonised with the gut microbiota from BPD-DS patients for 7 weeks. A non-metabolisable glucose analogue (3-O-methyl-D-glucopyranose (3-OMG), 4 mg/mouse) and paracetamol (1 mg/mouse) were gavaged to mice and quantified in circulation by high-pressure liquid chromatography equipped with a triple quadrupole mass spectrometer (see online supplemental material for further details).

Intestinal and vascular surgery

Rats were anaesthetised (ketamine, 60 mg/kg; xylazine, 8 mg/kg) prior to surgical procedures. Gut catheters were placed into the luminal compartment 6 cm and 18–22 cm distal to the pyloric sphincter and therefore positioned at the upper small intestine (USI) and middle jejunum, respectively. Alternatively, the middle jejunum catheters were replaced by more distal cannulation placed at the middle ileum (see online supplemental methods for details). For vascular surgery, catheters were implanted into the left carotid artery and right jugular vein for blood sampling. Postsurgical food intake and body weight were monitored daily for 5 days leading up to the experiment. Rats that did not attain at least 85% of their pre-USI/jejunal and vascular surgical body weight were excluded.

Human-to-rat faecal transplants and upper small intestine glucose tolerance test

Equivalent amounts of stool samples from BPD-DS donor patients were pooled together for each timepoint (ie, presurgery and postsurgery). Faecal slurries were obtained from combined stools before and after surgery as described in Donor patients and faecal slurries. One day following jejunal cannulation, freshly thawed slurries were directly infused into the jejunal cannula to target the distal jejunum and ileum of

Table 1 Donor patient characteristics

Patient	Surgery type	Age	BMI (kg/m^2)				Body weight (kg)				FBG (mmol/L)				HbA1c (%)			
			Presurgery	Postsurgery	Change (%)	P value	Presurgery	Postsurgery	Change (%)	P value	Presurgery	Postsurgery	Change (%)	P value	Presurgery	Postsurgery	Change (%)	P value
1	BPD-DS	56	46.9	28.5	−39.2		120	73	−39.2		11.5	5.6	−51.3		8.6	5.4	−37.2	
2		48	56.2	32.6	−42.0		162	92	−43.2		10	5.7	−43.0		7.6	4.3	−43.4	
3		52	50.1	29.7	−40.7		129.8	77	−40.7		8.3	6	−27.7		7.1	4.7	−33.8	
Mean±SD		52±4.0	51.1±4.7	30.3±2.1	−40.6±1.4	0.002	137.3±22	80.7±10	−41.0±2.0	0.01	9.9±1.6	5.8±0.2	−40.7±12.0	0.011	7.8±0.8	4.8±0.6	−38.1±4.9	0.006
1	LSG	44.8	35	23	−34.3		93	61	−34.4		7.3	5.8	−20.5		7	5.8	−17.1	
2		54	47	33.9	−27.9		131	94.5	−27.9		7	4.4	−37.1		5.6	5	−10.7	
3		39	49.9	36.3	−27.3		141.8	103	−27.7		7.2	5	−30.6		5.7	5.2	−8.8	
Mean±SD		46±7.5	44±7.9	31.1±7.1	−29.8±3.8	0.103	121.9±25.6	86±22	−30.0±3.8	0.13	7.2±0.2	5.1±0.7	−29.4±8.4	0.007	6.1±0.8	5.3±0.4	−12.2±4.4	0.208

Data postsurgery were obtained 12 months after bariatric procedure.
BMI, body mass index; BPD-DS, biliopancreatic diversion with duodenal switch; FBG, fasting blood glucose; HbA1, haemoglobin A1; LSG, laparoscopic sleeve gastrectomy.

SPF rats (1.5 mL/rat, 3 times/week for 4 weeks). On 3 weeks of colonisation, rats underwent surgery for USI and vascular cannulation. After 5 days of recovery (during which colonisation via jejunal cannula was maintained), rats were fasted overnight (16 hours, from 16:00 to 8:00 hours), and a bolus of phloridzin (P3449, Sigma-Aldrich, 0.04 g/kg) or vehicle (10% dimethyl sulfoxide and 10% ethanol in 0.9% saline) was infused via jejunal cannula (targeting distal jejunum and ileum) and was immediately followed by a bolus of glucose (G8769, Sigma-Aldrich, 4 g/kg) infusion into the USI cannula (targeting almost the entire small intestine). Blood glucose was monitored 0, 5, 10, 20, 30, 40 min after USI glucose infusion.

See online supplemental methods for details on metabolic phenotyping, bacterial profiling, histological analysis, messenger RNA (mRNA) extraction, RT-PCR analysis, immunoblotting and short-chain fatty acid determination.

Statistical analysis

Analysis of microbial populations was conducted in R. Partitioning of the variance in the microbiota was done with a permutational multivariate analysis of variance on Bray-Curtis dissimilarities calculated from relative amplicon sequence variant (ASV) abundances. The Wilcoxon rank-sum test was used for pairwise comparisons. Adjustment for the false discovery rate was calculated with the Benjamini-Hochberg method.[15] R packages used for data analysis and visualisation included phyloseq,[16] vegan,[17] UpsetR,[18] ggplot2,[19] tidyr,[20] dplyr,[21] ggtree[22] and corrplot.[23] Significance was accepted at $p<0.05$. Statistical analyses of other variables were done using unpaired two-tailed Student's t-test in GraphPad Prism V.9.

Data availability: all data and R scripts generated in this study are available on reasonable request. 16S rRNA gene sequencing data were deposited to the National Institutes of Health's Sequence Read Archive (temporary ID 124400).

RESULTS

Gut microbiota after bariatric surgery improves blood glucose control

Female patients had lower fasting blood glucose 12 months after LSG or BPD-DS (figure 1A, table 1). Faecal slurries from one donor patient before (presurgery) or 12 months after (postsurgery) each type of bariatric surgery were used to colonise two to five mice, and separate mice were used for testing the faeces from the same patient before and after surgery (figure 1B). GF mice, but not their SPF counterparts, had lower blood glucose and lower area under the curve (AUC) during a glucose tolerance test (GTT) following long-term (7 weeks) exposure to faecal samples from patients post-BPD-DS as compared with mice exposed for the same amount of time to patient faecal slurries before BPD-DS (figure 1C,D). We observed similar outcomes when faecal samples from LSG patients were used to colonise mice for 7 weeks, where lower blood glucose tolerance and lower AUC during a GTT was observed for GF, but not SPF mice, which received faeces from patients post-LSG as compared with mice exposed to patient faecal matter before LSG (figure 1E,F). This microbiota-transmissible improvement in glucose tolerance using faecal material after BPD-DS and LSG was not associated with changes in food intake or body composition in GF mice (online supplemental figure 1). We found that human-to-mouse faecal microbiota transmission of improved glucose tolerance postbariatric surgery was not attributable to a

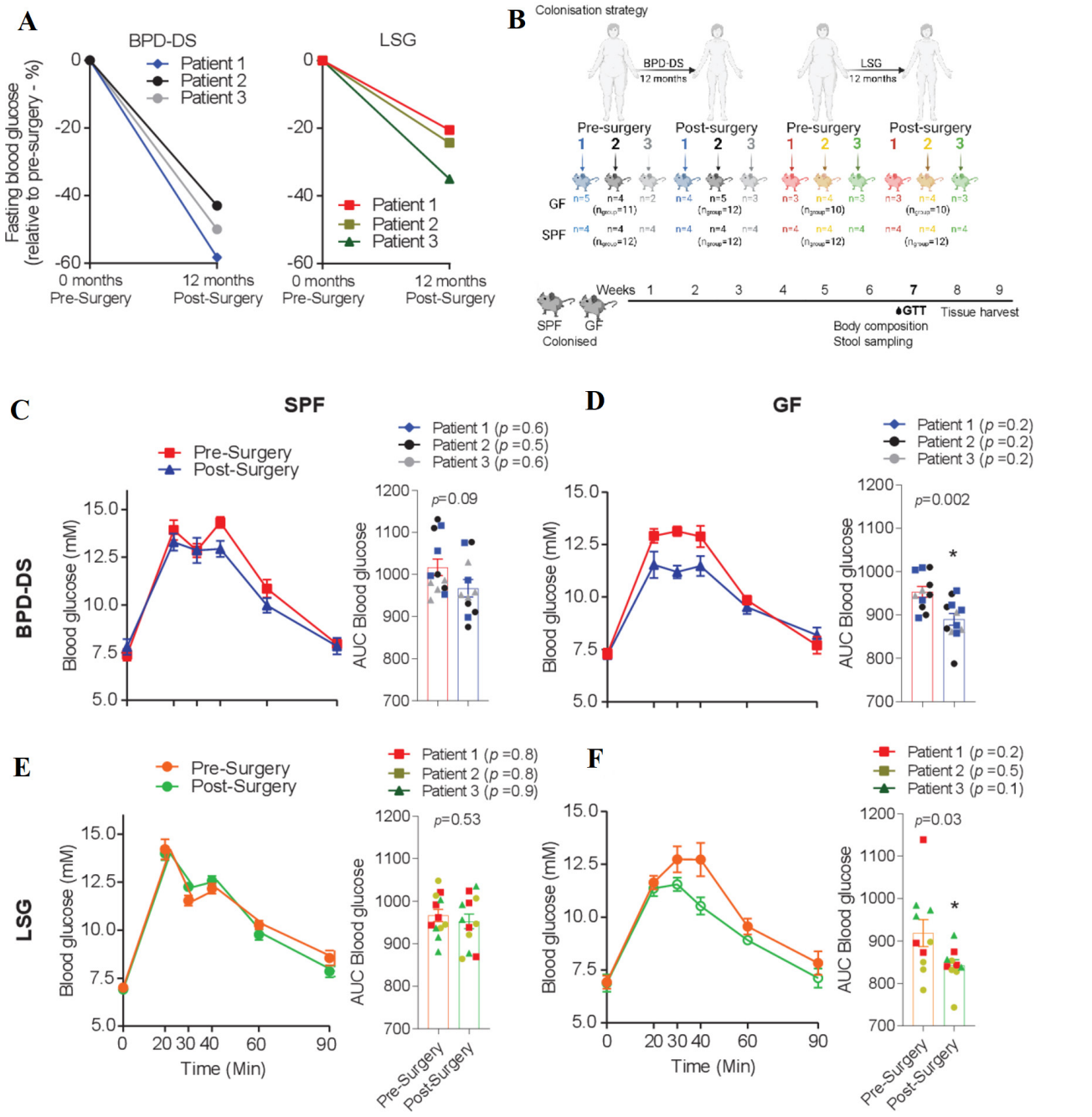

Figure 1 Glucose tolerance in mice colonised with the faecal microbiota of patients before and after different types of bariatric surgery. (A) Change in fasting blood glucose 12 months after bioliopancreatic diversion with duodenal switch (BPD-DS) or laparoscopic sleeve gastrectomy (LSG) in female donor patients. (B) Colonisation strategy and timeline of body feature assessment and metabolic profiling in female germ-free (GF) and specific pathogen-free (SPF) mice colonised with faecal slurries from female patients before and after different types of bariatric surgery. Glucose excursion curves and area under the curves (AUC) of oral glucose tolerance tests (GTT) performed in SPF and GF mice colonised with the faecal microbiota of patients before and after (C, D) BPD-DS and (E, F) LSG. Data are presented as the mean±SEM. Unpaired Student's t-test was used to calculate p values, which were considered significant at p<0.05 denoted by a *. Each square, triangle and circle represents a biological replicate (n=10–12). In AUC plots, each symbol colour represents a donor patient, and p values for within-donor comparisons of AUC in recipient mice presurgery versus postsurgery are described on the top of each panel next to the legend.

specific human patient (figure 1D,F—see in the legend at the top the p values for within-donor comparison of AUC during a GTT in mice). These data show that bariatric surgery-induced changes in the human microbiota within the same patient can transmit improved glucose tolerance to GF mice without changes in food intake or fat mass.

Gut microbiota after bariatric surgery lowers intestinal glucose absorption

To gain mechanistic insight into gut microbiota-mediated human-to-mouse transmission of improved glucose control, we first assessed glucose-stimulated insulin/c-peptide secretion (GSIS) and insulin sensitivity in GF mice colonised with

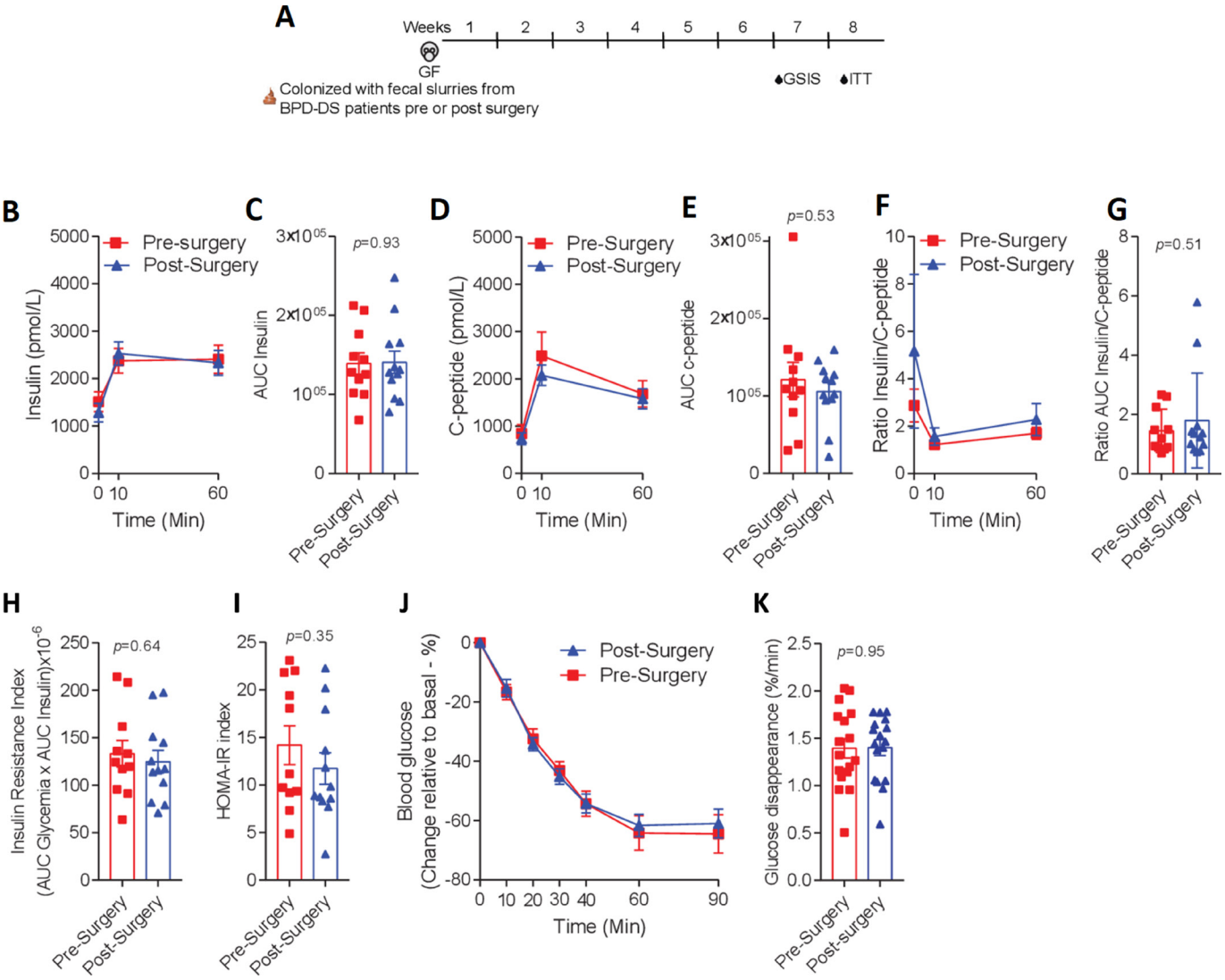

Figure 2 Glucose-stimulated insulin and c-peptide levels and insulin sensitivity in mice colonised with the faecal microbiota of patients before and after bioliopancreatic diversion with duodenal switch (BPD-DS). (A) Timeline of metabolic profiling in female germ-free (GF) mice colonised with faecal slurries from female patients before and after BPD-DS. (B, C) Plasma insulin, (D, E) c-peptide and (F, G) insulin/c-peptide ratio during glucose-stimulated insulin secretion (GSIS) tests and area under the curves (AUC) in colonised mice. (H) Insulin resistance index, (I) homeostasis model assessment-estimated insulin resistance (HOMA-IR), (J) glucose excursion curves during insulin tolerance tests (ITT) and (K) glucose disappearance rate during ITT in colonised mice. Data are presented as the mean±SEM. Unpaired Student's t-test was used to calculate p values, which were considered significant at p<0.05. Each square and triangle represents a biological replicate (B–H, n=11–12; J, K, n=16–17).

faeces before and after BPD-DS (figure 2A). Pre-BPD-DS and post-BPD-DS colonised mice had similar plasma insulin and c-peptide levels during GSIS (figure 2B–E) and similar insulin clearance, as measured by insulin/c-peptide ratio (figure 2F,G). Furthermore, pre-BPD-DS and post-BPD-DS recipient mice showed similar indices of insulin resistance, as measured by insulin resistance index (during the GTT) and homeostasis model assessment-estimated insulin resistance (figure 2H,I). Likewise, GF mice colonised with the microbiota before or after BPD-DS showed comparable blood glucose and glucose disappearance rate during an insulin tolerance test (figure 2J,K). No differences were found in SPF mice that received the faecal microbiota pre-BPD-DS or post-BPD-DS (online supplemental figure 2). These data show that improved glucose control in GF colonised with microbes after BPD-DS is not associated with changes in insulin secretion, clearance or sensitivity.

Previous studies have documented changes in intestinal glucose absorption associated with improved glycaemic homeostasis in Roux-en-Y Gastric Bypass (RYGB) and LSG.[24–28] However, it was unknown if bariatric surgery-induced changes in glucose absorption are linked to changes in the gut microbiota. We hypothesised that lower blood glucose during an oral glucose load in GF mice colonised with the microbiota from patients after BPD-DS was due to lower intestinal glucose absorption. We gavaged another cohort of GF mice colonised with the microbiota of BPD-DS patients before and after surgery with a non-metabolisable glucose analogue (3-OMG), to assess gut glucose absorption, and paracetamol, to assess gastric emptying (figure 3A). Consistent with lower intestinal glucose absorption, GF mice colonised with the microbiota after BPD-DS had lower rate of appearance of 3-OMG in circulation and lower peak 3-OMG serum concentration compared with mice colonised with

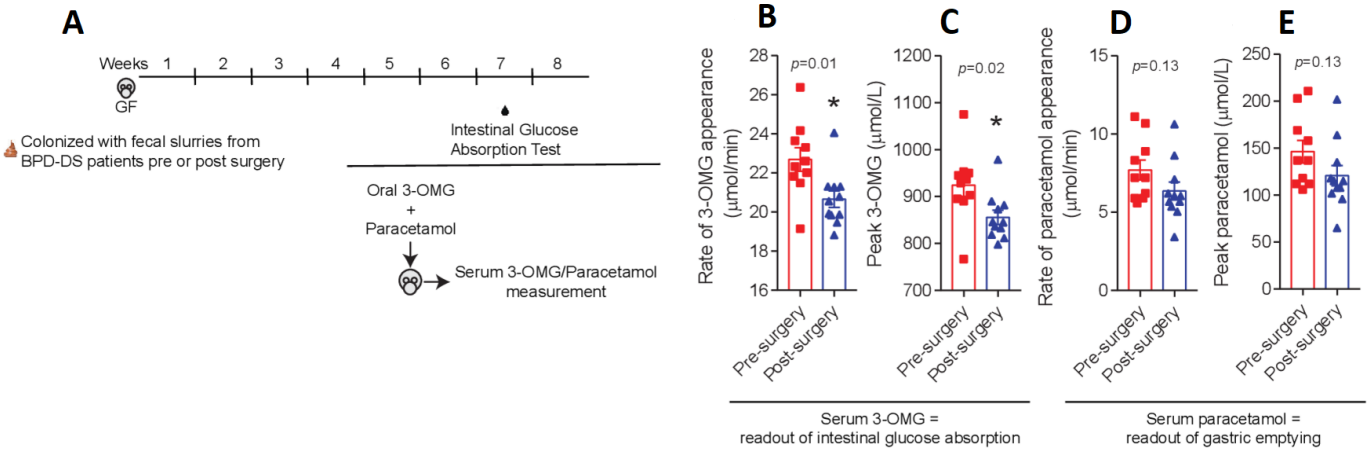

Figure 3 Intestinal glucose absorption in mice colonised with the faecal microbiota of patients before and after bioliopancreatic diversion with duodenal switch (BPD-DS). (A) Timeline and study design of intestinal glucose absorption tests performed in female germ-free (GF) mice colonised with faecal slurries from female patients before and after BPD-DS. Rate of appearance in circulation and plasma peak concentration of (B, C) 3-O-methyl-D-glucopyranose (3-OMG) and (D, E) paracetamol during intestinal glucose absorption tests. Data are presented as the mean±SEM. Unpaired Student's t-test was used to calculate p values, which were considered significant at p<0.05. Each square and triangle represents a biological replicate (B–E n=10–11).

presurgery microbes (figure 3B,C). GF mice colonised with either presurgery or postsurgery microbes had no change in gastric emptying indicated by a similar rate of appearance and peak levels of paracetamol in the serum (figure 3D,E).

The sodium-glucose cotransporter (Sglt)1 is the main glucose carrier from the lumen to the enterocyte. We next pharmacologically inhibited Sglt1 in mice colonised with gut microbes pre-LSG or post-LSG (figure 4A). We first performed oral GTT in naïve SPF mice to determine a dose of phloridzin that attenuated (but not eliminated) gut glucose absorption (online supplemental figure 3A–E). We showed that 0.04 g phloridzin/kg significantly lowered glucose entry through the gut during an oral glucose load, but not blood glucose clearance, since vehicle-treated and phloridzin-treated mice displayed comparable glucose tolerance on intraperitoneal GTT (online supplemental figure 3F, G). We then colonised an additional cohort of GF mice with faecal slurries pre-LSG or post-LSG and performed an oral GTT 1 hour after administration of vehicle or phloridzin. We confirmed that weight-matched vehicle-treated mice colonised with faecal slurries post-LSG had lower blood glucose than pre-LSG colonised mice (figure 4B,C and figure 1F); however, on Sglt1 inhibition, this difference was eliminated (figure 4D,E). These data show that Sglt1-mediated intestinal glucose absorption is a determinant of the glucose-lowering effect of gut microorganisms post-LSG.

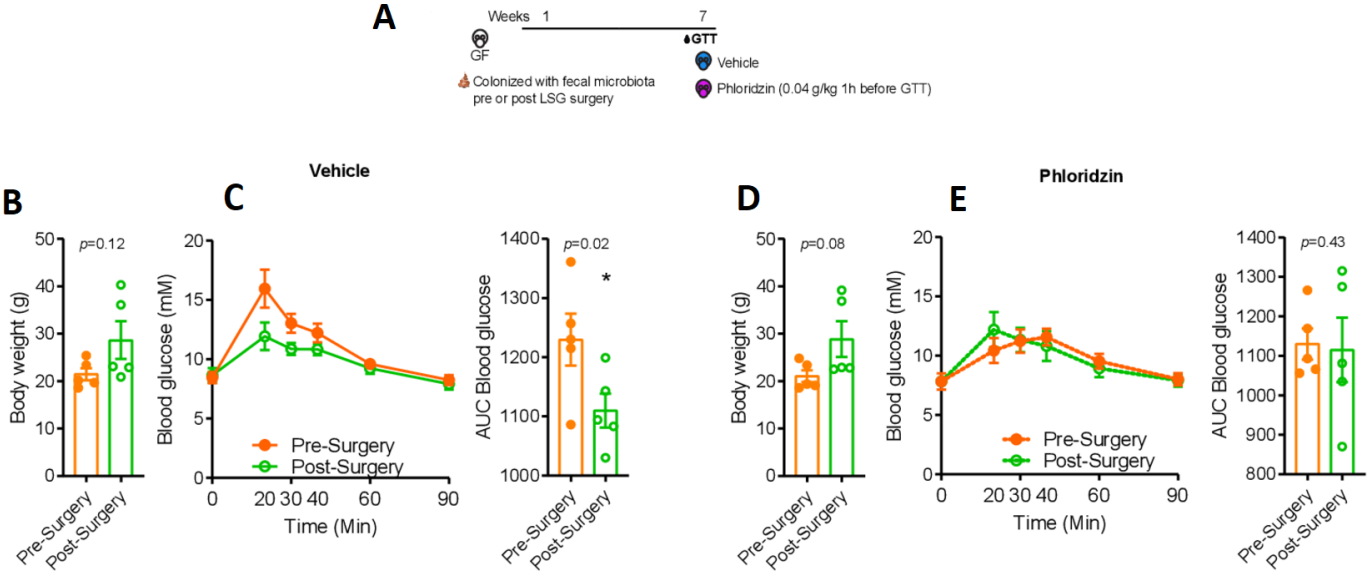

Figure 4 Inhibition of sodium-glucose cotransporter (Sglt)1 negates improved glucose tolerance in mice colonised with the faecal microbiota of patients after laparoscopic sleeve gastrectomy (LSG). (A) Female germ-free (GF) mice were colonised with the faecal microbiota of female patients before or after LSG and thereafter subjected to oral glucose tolerance tests (GTT) on inhibition of Sglt1 with phloridzin (0.04 g/kg). Body weight, glucose excursion curves and area under the curves (AUC) of oral GTT in mice injected with (B, C) vehicle and (D, E) phloridzin. Data are presented as the mean±SEM. Unpaired Student's t-test was used to calculate p values, which were considered significant at p<0.05. Each circle represents a biological replicate (n=5).

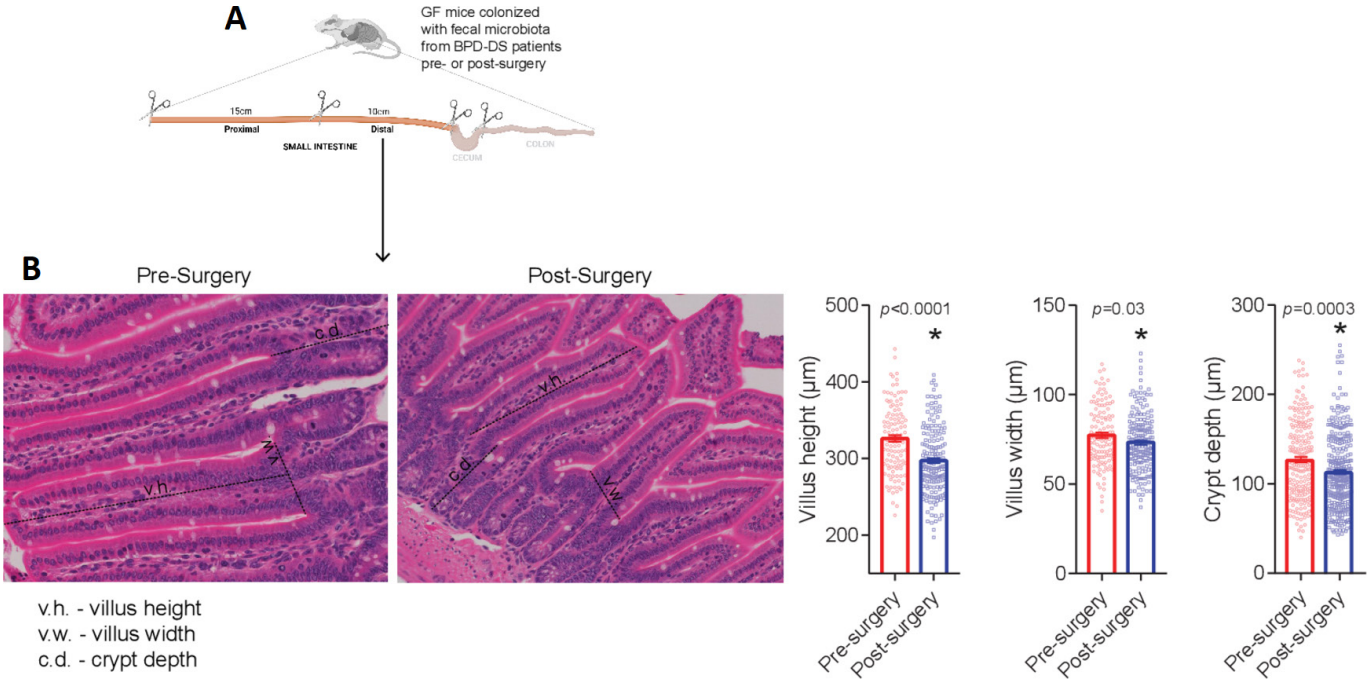

Figure 5 Morphological characteristics in the distal small intestine of mice colonised with the faecal microbiota of patients before and after bioliopancreatic diversion with duodenal switch (BPD-DS). (A) Schematic representation of method used to separate and harvest different intestinal sections from mice. (B) Representative images and morphometric analysis of H&E-stained distal small intestine sections harvested from female germ-free (GF) mice colonised with the faecal microbiota of female patients before and after BPD-DS. Each dot represents a villus or crypt (ie, technical replicates, n=115–324).

Gut microbiota post-BPD-DS alters gut morphology in recipient mice

We found no changes in *Slc5a1* (Sglt1), neither in *Slc2a1* (Glut1) and *Slc2a2* (Glut2), mRNA expression in the proximal and distal small intestine of GF mice colonised with gut microbes pre-BPD-DS or post-BPD-DS and LSG (online supplemental figure 4). Surprisingly, morphological analysis revealed that GF mice colonised with the microbiota after BPD-DS had lower villus height, villus width and crypt depth in the distal small intestine (figure 5A,B), but not in the proximal small intestine (online supplemental figure 5), as compared with GF mice that were colonised with the pre-BPD-DS microbiota.

Gut microbiota post-BPD-DS relays signals to the host via Wnt/β-catenin pathway

We next sought to determine possible mechanisms mediating lower villus height, villus width and crypt depth observed in the distal small intestine of GF mice harbouring gut microorganisms pre-BPD-DS or post-BPD-DS. Short-chain fatty acids (SCFAs) are key bacterial products involved in host physiological control, including enterocyte homeostasis. While BPD-DS donors had higher levels of faecal butyric acid and LSG donors displayed lower levels of faecal acetic acid postsurgery, these features were not recapitulated in caecal contents of colonised mice (online supplemental figure 6), suggesting that SCFA are not the main players in the changes in gut structure, intestinal absorption or blood glucose in mice.

The Wnt/β-catenin pathway is known to integrate signals to control enterocyte proliferation through activation of β-catenin (online supplemental figure 7A). The levels of active/inactive β-catenin were lower in the distal small intestine of mice colonised with slurries post-BPD-DS comparable in the distal small intestine of GF mice pre-BPD-DS (online supplemental figure 7B–E), but mice with microorganisms post-BPD-DS showed higher levels of inactive β-catenin than counterparts harbouring the microbiota pre-BPD-DS (online supplemental figure 7B). These findings suggest that the gut microbiota after BPD-DS can relay signals to the host and alter the activation status of β-catenin, which can potentially curb cell proliferation and possibly contribute to lower gut absorptive surface in intestinal cells exposed to the microbiota after bariatric surgery.

Targeted colonisation of the distal small intestine with the gut microbiota from patients post-BPD-DS lowers blood glucose in rats in a Sglt1-dependent manner

To test gut microbial-related changes directly in the distal small intestine in another model that already harbours a microbiota, we colonised female SPF rats by directly infusing faecal slurries from female patients before or after BPD-DS into the rat's distal small intestine followed by USI GTT (figure 6A). In weight-matched SPF rats (figure 6B), distal small intestinal colonisation with the gut microbiota from patients after BPD-DS was sufficient to lower blood glucose AUCs on USI-GTT compared with rats that received the faecal slurries pre-BPD-DS (figure 6C). With comparable pre-experimental body mass (figure 6D), this effect was negated by intrajejunal administration of phloridzin (figure 6E). To assess whether the distal small intestinal glucose absorption occurs in the ileum, glucose was infused into the ileum, instead of USI, of rats via ileal cannulation. We found that ileal glucose infusion failed to elevate blood glucose (online supplemental figure 8). These data suggest that gut microbes after BPD-DS can improve glucose tolerance in the host by locally reducing glucose absorption in the distal jejunum, but not the ileum, of SPF rats.

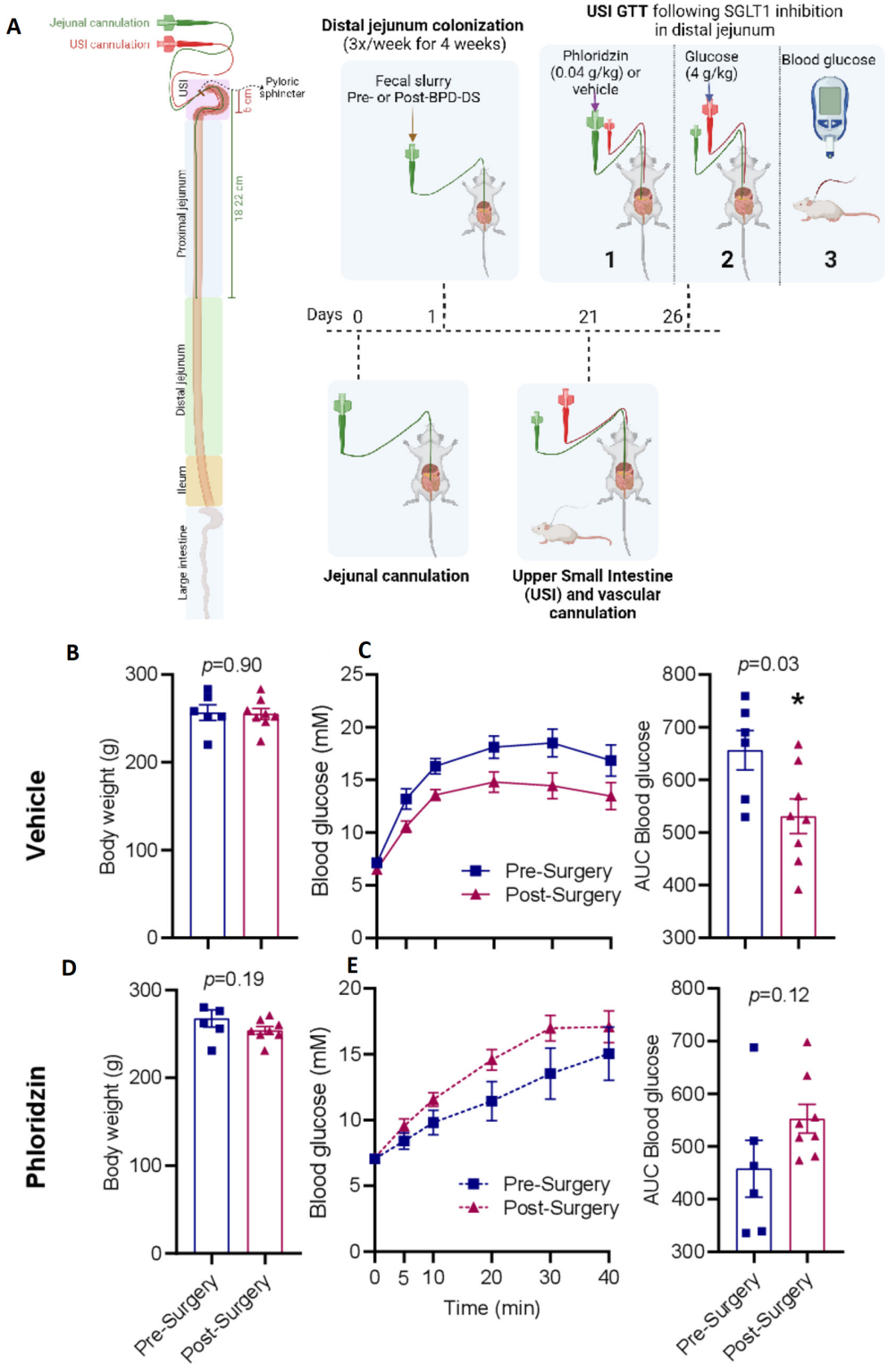

Figure 6 Targeted colonisation of the distal small intestine with gut microbes from patients after bioliopancreatic diversion with duodenal switch (BPD-DS) lowers blood glucose in rats in a sodium-glucose cotransporter (Sglt)1-dependent manner. (A) Gut catheters were placed into the luminal compartment of specific pathogen-free (SPF) female rats 6 cm and 18–22 cm distal to the pyloric sphincter and therefore positioned at the upper small intestine (USI) and middle jejunum, respectively. Next, 1 day after jejunal cannulation, equivalent amounts of faecal slurries from female patients before or after BPD-DS were pooled together and infused into the jejunal cannula 3 times a week for 4 weeks to target the distal jejunum and ileum of SPF rats. On 3 weeks (ie, 21 days) of colonisation, rats underwent surgery for USI and vascular cannulation. After 5 days of recovery, rats were fasted overnight, infused with vehicle or phloridzin via jejunal cannula (targeting the distal jejunum and ileum) and then immediately infused with glucose through the USI cannula (targeting almost the entire small intestine). Blood glucose was monitored at different time points (0, 5, 10, 20, 30, 40 min) after USI glucose infusion. Body weight, glucose excursion curves and area under the curves (AUC) of USI GTT in rats infused with (B, C) vehicle and (D, E) phloridzin. Data are presented as the mean±SEM. Unpaired Student's t-test was used to calculate p values, which were considered significant at $p<0.05$. Each square or triangle represents a biological replicate (n=6–8).

Specific taxonomic features in recipient mice post-BPD-DS and post-LSG are linked to microbiota-transmissible improvements in blood glucose control

To identify bacterial community characteristics transmitted from bariatric surgery patients to mice, we applied 16S rRNA gene-based sequencing analysis of faecal samples of GF colonised with the microbiota before and after LSG and BPD-DS. In our model, 7.3% and 18.7% of the ASVs identified in the stools of donor patients who underwent BPD-DS and LSG, respectively, were transmitted to recipient GF mice (online supplemental figure 9). The transmitted taxa represented 13.1% and 20% of all ASVs found in the BPD-DS and LSG recipient mice, respectively (online supplemental figure 9). Consistent with previous reports,[29 30] BPD-DS tended to lower α-diversity in donor patients (online supplemental figure 10A), which was not seen after LSG (online supplemental figure 10B). We found that α-diversity was not different in GF mice colonised with human faeces from BPD-DS and LSG patients (online supplemental figure 10C,D), indicating that microbial α-diversity in stool samples is not a key feature in human to mouse microbiota-mediated transmission of changes in blood glucose. These findings are in agreement with reports showing that improved glycaemic control postbariatric surgery is not associated with higher bacterial diversity.[30 31]

Principal component analysis of Bray-Curtis dissimilarity of the taxonomic composition of stool samples from mice colonised with faeces from BPD-DS or LSG patients showed no separation in the microbial community composition pre-BPD-DS and post-BPD-DS (figure 7A). Conversely, the microbial composition of the stool samples segregated pre-LSG and post-LSG, with 46.2% of the variation among samples explained by the first two axes (figure 7B). We further investigated abundance of taxa presurgery and post-surgery and found that post-LSG recipient stools had higher levels of *Parabacteroides* and several members of the class Clostridia (eg, *Caproiciproducens*, *Robinsoniella*, GCA-900066575) compared with pre-LSG recipients (figure 7C and online supplemental figure 11). *Blautia*, another member of the class Clostridia, was an exception and showed lower abundance in post-LSG recipients (figure 7C and online supplemental figure 11). For the BPD-DS recipients, we found a more subtle expansion of Clostridia characterised by higher presence of three taxa: *Robinsoniella*, GCA-900066575 (which were also higher in post-LSG recipients) and *Anaerostignum* (figure 7C and online supplemental figure 11). Similar to GF mice that were colonised with the microbiota after LSG, lower *Blautia* and elevated levels of *Parabacteroides* was also found in GF mice colonised with post-BPD-DS microbiota (figure 7C and online supplemental figure 11). Our findings highlight taxonomic features post-BPD-DS and post-LSG linked to microbiota-transmissible improvements in blood glucose control.

DISCUSSION

Our data show that a subset of gut microorganisms from patients after two different bariatric surgeries is associated with better glucose tolerance independently of changes in fat mass in mice. We found that the gut microbiota after restrictive and malabsorptive surgery in humans contain microbes (or microbial factors) that can lower blood glucose. However, we found that the microbiota after either bariatric surgery did not change insulin secretion, insulin clearance or insulin resistance. We found that the mechanism for lower blood glucose caused by the microbiota after bariatric surgery was a lower intestinal glucose absorption in the distal small intestine. This is important because patients with morbid obesity have increased intestinal glucose absorption.[32] It was already known that bariatric surgery, such as BPD-DS, promotes glucose excretion into the gut lumen[28] and increases enterocyte hyperplasia/hypertrophy and glycolysis, rendering the intestine a key site for blood glucose disposal.[25–27 33] However, while these adaptive changes typical of malabsorptive surgery are not present in LSG patients, lower intestinal glucose absorption is still seen following restrictive procedures.[26 27] Here, we show that bacteria after bariatric surgery are a standalone factor that can lower the host's enteric absorptive surface, and lower postprandial glucose absorption in the gut. There is a precedent for gut microorganisms and diet regulating intestinal morphology. Probiotic bacteria can modify intestinal morphology in fish,[34] and high fat-fed mice have lower gut absorptive surface.[35] It is enticing to speculate that certain gut microorganisms after bariatric surgery in humans, may exert counter-regulatory pressure as a means to compensate for enterocyte hyperplasia/hypertrophy after malabsorptive surgery,[25] which, in light of our findings, may engage the Wnt/β-catenin pathway to relay signals to the host upper intestine.

The microbiota composition rapidly changes after bariatric surgery.[6] We initially hypothesised that changes in microbes would participate in blood glucose lowering early after bariatric surgery, such as the first few days before significant weight loss. However, our data raise the intriguing possibility that the function of microbes may be to improve long-term blood glucose control rather than the immediate effects of bariatric surgery. In our study, we used germ-free mice colonised for at least 7 weeks since sufficient exposure time (ie, >45 days) and multiple instillations by gavage are required for microorganisms to influence blood glucose in GF mice.[36 37] Modest improvements in glucose homeostasis after faecal microbial transplants into mice from rats that underwent RYGB have been reported after short periods of time.[14] While this can be in part explained by differences in human BPD-DS compared with rat RYGB,[8] exposure time of the host to certain microbes appears to be a key factor in altering blood glucose.

In our hands, colonisation via oral gavage of SPF mice with gut microbiota before and after bariatric surgery failed to transmit better glucose tolerance. However, we discovered that long-term (3 times/week for 4 weeks) direct intraluminal microbial transplantation into the distal small intestine of SPF rats can circumvent this limitation and transmit lower blood glucose using faecal bacteria after bariatric surgery. These findings set the stage to enhance microbial transplant protocols that can alter host metabolism. Overall, our work positions microbiota-induced changes in intestinal morphology and glucose absorption as a factor that could contribute to durable lowering of blood glucose and long-term T2D remission.

Amplicon-based methods, like the one used herein, do not allow an in-depth appreciation of colonisation efficiency, nor strain-level resolution of microbiota engraftment. Limitations considered, colonisation efficiency in our model was estimated to vary between 7% and 20%, which is lower than previously reported.[12 37] We acknowledge that only a fraction of the donor microbiota is expected to survive sample collection, preparation/storage (eg, freeze-and-thaw cycles, exposure to oxygen) and delivery in our colonisation model. But most importantly, we showed that a relatively small subset of bacteria coming from the gut microbiota after two different types of bariatric surgery was sufficient to lower blood glucose in different rodent models. It is important to consider that (i) the human inocula before and after surgery were from the same patient and were processed equally, (ii) microbiota-transmissible improved glucose tolerance was seen in multiple cohorts of GF mice and in SPF rats and

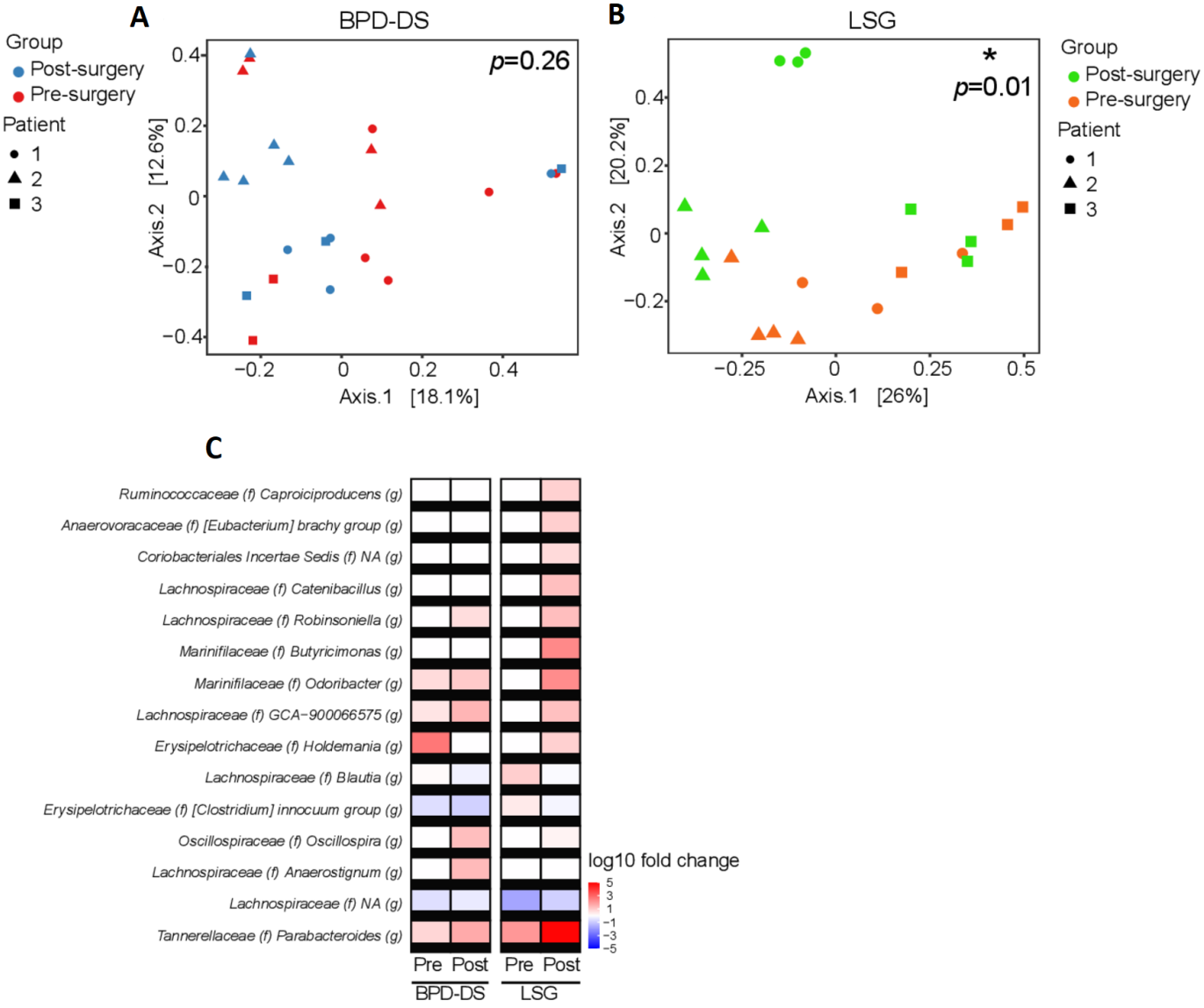

Figure 7 Bacterial composition of the faeces of mice colonised with the faecal microbiota of patients before and after bioliopancreatic diversion with duodenal switch (BPD-DS) or laparoscopic sleeve gastrectomy (LSG). (A, B) Principal coordinate analysis (PCoA) on Bray-Curtis dissimilarity index comparing the faecal bacterial composition of female germ-free (GF) mice colonised with the faecal microbiota of patients before and after BPD-DS or LSG. The samples are stratified by patient donors of faecal microbiota. Permutational multivariate analysis of variance was used to assign statistical significance to the distance between clusters (presurgery vs postsurgery) in PCoA scatter plots. (C) Heat maps depicting the average of replicates for taxa significantly different between presurgery and postsurgery groups ($p<0.05$, Wilcoxon rank-sum test). ASVs were clustered at 99% similarity and collapsed to the genus level. The relative abundance of taxa is expressed as $\log_{10}$ fold change from its median level across the entire cohort (both surgeries combined). All relative abundance values of 0 were assigned 1×10^{-6}, an order of magnitude lower than the lowest detectable relative abundance in the data, to allow the logarithmic transformation of the fold change. Each square, triangle and circle represents a biological replicate (n=11–12).

(iii) mouse and rat studies were performed by different operators in different animal facilities. While we could capitalise on this relatively small colonisation efficiency to narrow down the bacteria possibly implicated in lowering blood glucose in the host, it is important to acknowledge that our donor cohort was not big enough to allow a more precise identification of bacterial signatures in recipient mice. Each mouse was colonised with the faecal matter from one donor, and therefore the recipient mouse cohort reflected the high interindividual variability typically seen in the microbiota of human individuals. Importantly, we showed that transmission of improved glucose tolerance via microbiota transfer was not donor-specific, indicating that the diverse set of microbial communities that can occur in humans after different types of bariatric surgeries contain functional redundancies that can lower intestinal glucose absorption and blood glucose in the host.

Higher *Parabacteroides* and lower *Blautia* were among the key transmissible taxonomic features shared after restrictive and malabsorptive procedures and that coincided with better glucose control in recipient mice. We highlight these taxa because they were among the top 20 most abundant in the faeces of recipient mice and because previous findings have linked increased *Parabacteroides* spp with improved metabolic function during obesity.[38] Our results agree with Ridaura *et al*, where the microbes in lean/normoglycaemic humans can override an obese phenotype in GF mice colonised with faecal material from twin

pairs discordant for obesity. In particular, *Bacteroides* spp and *Parabacteroides* spp in lean-associated microbiota could colonise mice harbouring the microbiota associated with obesity.[12] An alternative approach to using twin pairs is to use within-patient comparison before and after bariatric surgery as we have done here, where a robust reduction in body weight and blood glucose is observed (table 1). Our results expand this concept and show that microbiota transmissible alterations in host metabolism associated with *Parabacteroides* spp can lower blood glucose without lowering body mass. It is noteworthy that *Parabacteroides* spp and the closely related genus *Bacteroides* exhibit underacylated lipopolysaccharide (LPS) that can antagonise toll-like receptor 4[39–41] and polysaccharide A with tolerogenic potential,[39 41 42] which may contribute to improved glucose tolerance in recipient mice postsurgery. Our data also point to *Blautia* as a common microbiota genus of improved blood glucose control postbariatric surgery. Indeed, *Blautia* was found to be higher in the faeces of individuals with diabetes[43 44] and lower after bariatric surgery.[6 29] Overall, our findings highlight that small groups of bacteria were consistently associated with transmission of improved blood glucose tolerance after two types of bariatric surgery. Since postbiotics can improve glucose homeostasis in the host,[45–48] we believe our work provide foundational evidence to support research on postbiotics that can lower intestinal glucose absorption and blood glucose. As a perspective, it is enticing to explore the link between mucosal serotonin and the microbiota-related glucose-lowering effects of bariatric surgery in follow-up studies. Gut-derived serotonin secretion is a microbiota-influenced trait[49] that has been shown to impact glucose regulation[50] and gut morphology.[51] In addition, while we showed that the human microbiota from women could transmit changes in blood glucose in female mice, any sex-dependent effect in males is not yet known.

We conclude that microorganisms in human faeces after bariatric surgery are a standalone factor that lowers Sglt1-mediated intestinal glucose absorption and consequently improves blood glucose control when transferred to rodents. This microbiota-driven effect is associated with structural changes in the villi of the distal small intestine. We propose a model where changes in microbiota contribute to the long-term glucose-lowering effects of bariatric surgery, independently of microbiota-related changes in obesity and insulin resistance. Microorganisms, and/or their components, that can lower glucose absorption should be mined as factors that can contribute to durable lowering of blood glucose by limiting entry of glucose into the host.

Author affiliations
[1]Department of Biochemistry and Biomedical Sciences, Farncombe Family Digestive Health Research Institute, and Centre for Metabolism, Obesity and Diabetes Research, McMaster University, Hamilton, Ontario, Canada
[2]Department of Genetics and Medicine, Stanford University, Stanford, California, USA
[3]Toronto General Hospital Research Institute, University Health Network, Toronto, Ontario, Canada
[4]Quebec Heart and Lung Institute Research Centre, Laval University, Quebec, Quebec, Canada
[5]Department of Medicine, Farncombe Family Digestive Health Research Institute, and Centre for Metabolism, Obesity and Diabetes Research, McMaster University, Hamilton, Ontario, Canada
[6]School of Nutrition, Laval University, Quebec, Quebec, Canada

Twitter Fernando F Anhê @fernando_anhe, Béatrice So-Yun Choi @BeatriceSY_Choi, Tony K T Lam @TKTLam and Jonathan Schertzer @SchertzerLab

Acknowledgements We are thankful to Mélissa Pelletier and Mélanie Nadeau for technical assistance with human data and samples, and to Nicola Henriquez for technical assistance with mass spectrometry.

Contributors FFA, JS, AM, TKTL and AT derived the hypothesis and researched the data. FFA conducted experiments, analysed the data and wrote the manuscript. SZ and S-YZ conducted experiments and analysed the data. BS-YC and NGB conducted experiments. CYC and KPF helped with experiments. LB performed surgeries. JS, AM and TKTL edited the manuscript. All authors contributed with data discussion and approved the manuscript prior to its submission. JS is the guarantor.

Funding This study was supported by a team grant from the Canadian Institutes of Health Research (CIHR) on bariatric care (TB2-138776), an Investigator-initiated study grant from Johnson & Johnson Medical Companies (Grant ETH-14-610) and a CIHR Canadian Microbiome Initiative 2 (CMI2) team grant (MRT-168045).

Disclaimer Funding sources for the trial had no role in the design, conduct or management of the study, in data collection, analysis or interpretation of data, or in the preparation of the present manuscript and decision to publish.

Competing interests FFA and S-YZ have Canadian Institutes of Health Research (CIHR) postdoctoral fellowships. AT and LB are recipients of research grant support from Johnson & Johnson Medical Companies, Bodynov and Medtronic for studies on bariatric surgery and the Research Chair in Bariatric and Metabolic Surgery at IUCPQ and Laval University. TKTL holds a Canada Research Chair in Diabetes and Obesity and a JK. McIvor endowed chair in Diabetes Research. JS holds a Canada Research Chair in Metabolic Inflammation. AM was supported by a CIHR/Pfizer research Chair in the pathogenesis of insulin resistance and cardiovascular diseases. JS is the guarantor of the study and, as such, assumes full responsability for the work and conduct of the study.

Patient and public involvement Patients and/or the public were involved in the design, or conduct, or reporting, or dissemination plans of this research. Refer to the 'Methods' section for further details.

Patient consent for publication Not applicable.

Ethics approval This study was approved by Québec Heart and Lung Institute Research Ethics Committee (protocol n° 2015-2466, 21160 and 21181, MP-10-2015-2489). All animal procedures were approved by McMaster University Animal Ethics Review Board (AREB, ref# 200103) and Institutional Animal Care and Use Committee at the University Health Network (UHN, ref# 5884.16) in accordance with the Canadian Council on Animal Care guidelines. Participants gave informed consent to participate in the study before taking part.

Provenance and peer review Not commissioned; externally peer reviewed.

Data availability statement Data are available on reasonable request.

ORCID iDs
Fernando F Anhê http://orcid.org/0000-0003-1543-4154
Béatrice So-Yun Choi http://orcid.org/0000-0001-8160-9448
André Tchernof http://orcid.org/0000-0002-2587-1000
Tony K T Lam http://orcid.org/0000-0003-2908-3324
Andre Marette http://orcid.org/0000-0003-3950-5973
Jonathan Schertzer http://orcid.org/0000-0002-1547-5856

REFERENCES

1 Wilkinson L, Yi N, Mehta T, *et al*. Development and validation of a model for predicting incident type 2 diabetes using quantitative clinical data and a Bayesian logistic model: a nationwide cohort and modeling study. *PLoS Med* 2020;17:e1003232.
2 Gurka MJ, Golden SH, Musani SK, *et al*. Independent associations between a metabolic syndrome severity score and future diabetes by sex and race: the Atherosclerosis risk in Communities study and Jackson heart study. *Diabetologia* 2017;60:1261–70.
3 Mingrone G, Panunzi S, De Gaetano A, *et al*. Bariatric surgery versus conventional medical therapy for type 2 diabetes. *N Engl J Med* 2012;366:1577–85.
4 Rao Kondapally Seshasai S, Kaptoge S, Thompson A, *et al*. Diabetes mellitus, fasting glucose, and risk of cause-specific death. *N Engl J Med* 2011;364:829–41.

5 Wiggins T, Guidozzi N, Welbourn R, *et al*. Association of bariatric surgery with all-cause mortality and incidence of obesity-related disease at a population level: a systematic review and meta-analysis. *PLoS Med* 2020;17:e1003206.
6 Anhê FF, Varin TV, Schertzer JD, *et al*. The gut microbiota as a mediator of metabolic benefits after bariatric surgery. *Can J Diabetes* 2017;41:439–47.
7 Kapeluto J, Tchernof A, Biertho L. Surgery for diabetes: clinical and mechanistic aspects. *Can J Diabetes* 2017;41:392–400.
8 Harris L-A, Kayser BD, Cefalo C, *et al*. Biliopancreatic diversion induces greater metabolic improvement than Roux-en-Y gastric bypass. *Cell Metab* 2019;30:855–64.
9 Liou AP, Paziuk M, Luevano JM, *et al*. Conserved shifts in the gut microbiota due to gastric bypass reduce host weight and adiposity. *Sci Transl Med* 2013;5:178ra41.
10 Tremaroli V, Karlsson F, Werling M, *et al*. Roux-En-Y gastric bypass and vertical banded gastroplasty induce long-term changes on the human gut microbiome contributing to fat mass regulation. *Cell Metab* 2015;22:228–38.
11 Liu Z, Coales I, Penney N, *et al*. A subset of Roux-en-Y gastric bypass bacterial Consortium Colonizes the gut of nonsurgical rats without inducing host-microbe metabolic changes. *mSystems* 2020;5. doi:10.1128/mSystems.01047-20. [Epub ahead of print: 08 12 2020].
12 Ridaura VK, Faith JJ, Rey FE, *et al*. Gut microbiota from twins discordant for obesity modulate metabolism in mice. *Science* 2013;341:1241214.
13 Asnicar F, Berry SE, Valdes AM. Microbiome connections with host metabolism and habitual diet from 1,098 deeply phenotyped individuals. *Nat Med* 2021:1–12.
14 Arora T, Seyfried F, Docherty NG, *et al*. Diabetes-Associated microbiota in fa/fa rats is modified by Roux-en-Y gastric bypass. *Isme J* 2017;11:2035–46.
15 Benjamini Y, Hochberg Y. Controlling the false discovery rate: a practical and powerful approach to multiple testing. *Journal of the Royal Statistical Society: Series B* 1995;57:289–300 http://www.jstor.org/stable/2346101
16 McMurdie PJ, Holmes S. phyloseq: an R package for reproducible interactive analysis and graphics of microbiome census data. *PLoS One* 2013;8:e61217.
17 VEGAN DP. A package of R functions for community ecology. *J Veg Sci* 2003;14:927–30.
18 Conway JR, Lex A, Gehlenborg N. UpSetR: an R package for the visualization of intersecting sets and their properties. *Bioinformatics* 2017;33:2938–40.
19 Wickham H. ggplot2. *Wiley Interdiscip Rev Comput Stat* 2011;3:180–5.
20 Wickham H, Wickham MH. Package 'tidyr'. Easily Tidy Data with'spread'and'gather ()'Functions 2017.
21 Mailund T. Manipulating data frames: dplyr. In: *R Data Science Quick Reference*. *Springer* 2019:109–60.
22 Yu G, Smith DK, Zhu H, *et al*. ggtree : an r package for visualization and annotation of phylogenetic trees with their covariates and other associated data. *Methods Ecol Evol* 2017;8:28–36.
23 Wei T, Simko V, Levy M. Package 'corrplot'. *Statistician* 2017;56:e24.
24 Baud G, Daoudi M, Hubert T, *et al*. Bile diversion in Roux-en-Y gastric bypass modulates sodium-dependent glucose intestinal uptake. *Cell Metab* 2016;23:547–53.
25 Saeidi N, Meoli L, Nestoridi E, *et al*. Reprogramming of intestinal glucose metabolism and glycemic control in rats after gastric bypass. *Science* 2013;341:406–10.
26 Cavin J-B, Couvelard A, Lebtahi R, *et al*. Differences in alimentary glucose absorption and intestinal disposal of blood glucose after Roux-en-Y gastric bypass vs sleeve gastrectomy. *Gastroenterology* 2016;150:454–64.
27 Mumphrey MB, Hao Z, Townsend RL, *et al*. Sleeve gastrectomy does not cause hypertrophy and reprogramming of intestinal glucose metabolism in rats. *Obes Surg* 2015;25:1468–73.
28 Kwon IG, Kang CW, Park J-P, *et al*. Serum glucose excretion after Roux-en-Y gastric bypass: a potential target for diabetes treatment. *Gut* 2021;70:1847-1856.
29 Patrone V, Vajana E, Minuti A, *et al*. Postoperative changes in fecal bacterial communities and fermentation products in obese patients undergoing bilio-intestinal bypass. *Front Microbiol* 2016;7:200.
30 Mukorako P, Lopez C, Baraboi E-D, *et al*. Alterations of gut microbiota after biliopancreatic diversion with duodenal switch in Wistar rats. *Obes Surg* 2019;29:2831–42.
31 Aron-Wisnewsky J, Prifti E, Belda E, *et al*. Major microbiota dysbiosis in severe obesity: fate after bariatric surgery. *Gut* 2019;68:70–82.
32 Nguyen NQ, Debreceni TL, Bambrick JE, *et al*. Accelerated intestinal glucose absorption in morbidly obese humans: relationship to glucose transporters, incretin hormones, and glycemia. *J Clin Endocrinol Metab* 2015;100:968–76.
33 Murray ME, Franks G, Gazet J-C, *et al*. Radiologic demonstration of small bowel adaptation following modified Scopinaro procedure for morbid obesity. *Obes Surg* 1993;3:165–8.
34 Asaduzzaman MD, Iehata S, Akter S, *et al*. Effects of host gut-derived probiotic bacteria on gut morphology, microbiota composition and volatile short chain fatty acids production of Malaysian Mahseer TOR tambroides. *Aquaculture Reports* 2018;9:53–61.
35 Navarrete J, Vásquez B, Del Sol M. Morphoquantitative analysis of the ileum of C57BL/6 mice (Mus musculus) fed with a high-fat diet. *Int J Clin Exp Pathol* 2015;8:14649.
36 Foley KP, Zlitni S, Denou E, *et al*. Long term but not short term exposure to obesity related microbiota promotes host insulin resistance. *Nat Commun* 2018;9:4681.
37 Choo JM, Rogers GB. Gut microbiota transplantation for colonization of germ-free mice. *STAR Protoc* 2021;2:100610.
38 Wang K, Liao M, Zhou N, *et al*. Parabacteroides distasonis alleviates obesity and metabolic dysfunctions via production of succinate and secondary bile acids. *Cell Rep* 2019;26:222–35.
39 Vatanen T, Kostic AD, D'Hennezel E, *et al*. Variation in microbiome LPS immunogenicity contributes to autoimmunity in humans. *Cell* 2016;165:842–53.
40 Yoshida N, Emoto T, Yamashita T, *et al*. Bacteroides vulgatus and Bacteroides dorei reduce gut microbial lipopolysaccharide production and inhibit atherosclerosis. *Circulation* 2018;138:2486–98.
41 Hiippala K, Kainulainen V, Suutarinen M, *et al*. Isolation of Anti-Inflammatory and Epithelium Reinforcing *Bacteroides* and *Parabacteroides* Spp. from A Healthy Fecal Donor. *Nutrients* 2020;12:935.
42 Erturk-Hasdemir D, Oh SF, Okan NA, *et al*. Symbionts exploit complex signaling to educate the immune system. *Proc Natl Acad Sci U S A* 2019;116:26157–66.
43 Lippert K, Kedenko L, Antonielli L, *et al*. Gut microbiota dysbiosis associated with glucose metabolism disorders and the metabolic syndrome in older adults. *Benef Microbes* 2017;8:545–56.
44 Egshatyan L, Kashtanova D, Popenko A, *et al*. Gut microbiota and diet in patients with different glucose tolerance. *Endocr Connect* 2016;5:1–9.
45 Cavallari JF, Schertzer JD. Intestinal microbiota contributes to energy balance, metabolic inflammation, and insulin resistance in obesity. *J Obes Metab Syndr* 2017;26:161–71.
46 Cavallari JF, Pokrajac NT, Zlitni S, *et al*. Nod2 in hepatocytes engages a liver-gut axis to protect against steatosis, fibrosis, and gut dysbiosis during fatty liver disease in mice. *Am J Physiol Endocrinol Metab* 2020;319:E305–14.
47 Cavallari JF, Fullerton MD, Duggan BM, *et al*. Muramyl dipeptide-based Postbiotics mitigate obesity-induced insulin resistance via IRF4. *Cell Metab* 2017;25:1063–74.
48 Cavallari JF, Barra NG, Foley KP, *et al*. Postbiotics for NOD2 require nonhematopoietic RIPK2 to improve blood glucose and metabolic inflammation in mice. *Am J Physiol Endocrinol Metab* 2020;318:E579–85.
49 Yano JM, Yu K, Donaldson GP, *et al*. Indigenous bacteria from the gut microbiota regulate host serotonin biosynthesis. *Cell* 2015;161:264–76.
50 Martin AM, Yabut JM, Choo JM, *et al*. The gut microbiome regulates host glucose homeostasis via peripheral serotonin. *Proc Natl Acad Sci U S A* 2019;116:19802–4.
51 Heredia DJ, Gershon MD, Koh SD, *et al*. Important role of mucosal serotonin in colonic propulsion and peristaltic reflexes: in vitro analyses in mice lacking tryptophan hydroxylase 1. *J Physiol* 2013;591:5939–57.

Supplemental material

Human gut microbiota after bariatric surgery alters intestinal morphology and glucose absorption in mice independent of obesity

Supplemental Methods

Bariatric surgical procedure. Laparoscopic Sleeve Gastrectomy **(**LSG) was performed following removal of the greater curvature and fundus of the stomach. Briefly, the greater curvature of the stomach was mobilized from the antrum to the Hiss angle. A gastric tube was therefore created using repeated 60mm firing of linear staplers/cutters over a 34-French bougie, starting 5cm from the pylorus to the Hiss angle. Bilio-Pancreatic Diversion with a Duodenal Switch (BPD-DS) was carried out following a LSG created along a 34-French bougie, starting 7 cm from the pylorus. In addition, the duodenum was transected 3 cm distal to the pylorus and anastomosed to a 250 cm alimentary limb with a 100 cm common channel. Duodeno-ileal anastomosis was hand-sewn, whereas ileo-ileal anastomosis was semi-mechanical.

Ileal surgery and ileal glucose infusion. Male rats were anaesthetized (ketamine, 60 mg/kg; xylazine, 8 mg/kg) prior to surgical procedures. Gut catheters were placed into the luminal compartment 2 cm distal to the ileocecal valve. Vascular surgeries were performed as described in the 'Intestinal and vascular surgery' part of 'Material & Methods' section. After four days of recovery, rats were fasted overnight (16h, from 16:00 to 8:00) and a bolus of glucose at 2 different doses (0.25 or 4 g/kg) was infused via the ileal catheter. Blood glucose was monitored at different time points (0, 20, 30, 40 min) after ileal glucose infusion.

Anhê FF, *et al. Gut* 2022;0:1–12. doi: 10.1136/gutjnl-2022-328185

*Mass spectrometry***.** To assess circulating 3-OMG in circulation, deproteinised plasma samples were derivatised by acetylation and injected into an Agilent 1290 Infinity II HPLC with an Agilent 6495C iFunnel QQQ mass spectrometer for detection. Analytes were separated on an Agilent RRHD Eclipse Plus C18 (100 mm x 2.1 mm, i.d., 1.8 µm) column using mobile phases consisting of (A) 0.1% (v/v) formic acid in water and (B) 0.1% (v/v) formic acid in acetonitrile and a constant flow of 0.4 mL/min. For Paracetamol quantification, deproteinised samples were injected into the same equipment using the same column and mobile phases and a constant flow of 0.3 mL/min. Autosampler and column were maintained at 10˚C and 30 ˚C, respectively, throughout the analysis.

Short-chain Fatty Acids (SCFA). SCFA were assessed in the fæces of donor patients and in the cecal content of germ-free mice colonized with the the fecal microbiota of patients pre- or post-LSG or BPD-DS. Immediately after collection, fæces were weighed and 1 mL of distilled water/100 mg of material was added. Fecal suspensions were homogenized for 2 min with a Bead Ruptor 12 (Omni International, Kennesaw, GA, USA) and centrifuged at 18,000 × *g* for 10 min at 4 °C. The supernatant was collected, and an equal volume of ethyl acetate spiked with internal standard 4-methylvaleric acid was added and samples were acidified with phosphoric acid 10%. To extract SCFA, samples were mixed 2 min at 2400 rpm using a VWR VX-2500 Multitube Vortexer (VWR, Radnor, PA, USA), then centrifuged at 18,000 × *g* for 10 min at 4 °C. The organic phase was transferred to an autosampler vial for gas chromatography analysis. A 5-point calibration curve were prepared with a mix of acetic acid, propionic acid, butyric acid, isobutyric acid, valeric acid, isovaleric acid, and internal standard 4-methylvaleric acid. SCFA quantification was performed on a Shimadzu GC 2010 Plus equipped with a Nukol Supelco capillary GC column (30 m × 0.25 mm id, 0.25 µm) and a FID detector.

Histology. Proximal (ie, ~15 cm distal to the pylorus) and distal (ie, ~10 cm proximal to ileocecal sphincter) small intestine were arranged in Swiss-rolls and fixed in Carnoy's solution containing ethanol, chloroform and glacial acetic acid (6:3:1) for 3 h. After thorough washing in 100% ethanol, samples were immersed in 70% ethanol for 72 hours. Five µm cross-sections were mounted onto slides and stained with hematoxylin and eosin (H&E). Images of H&E-stained slides were acquired with a Nikon Eclipse Ni & DS-QI2 microscope and analyzed using NIS-Elements. Morphometry was conducted with Image J.

Messenger RNA extraction and RT qPCR. Total RNA was obtained from ~50 mg of upper or distal small intestine via mechanical homogenization at 4.5 m/s for 30 s using a FastPrep-24 tissue homogenizer (MP Biomedicals) and glass beads in tryzol. RNA was extracted using the Directzol RNA Miniprep kit (Zymo Research) and cDNA synthesis was made from 1 µg of tissue RNA using High Capacity cDNA Reverse Transcriptase kit (Applied Bioscience). Transcript expression was measured using TaqMan Assays with AmpliTaq Gold DNA polymerase (Thermo Fisher Scientific). The ΔΔCt for target genes was calculated using 18S as a reference gene. The following primers were used in this study: Glut1 (*Slc2a1*, Mm00441480_m1), Glut2 (*Slc2a2*, Mm00446229_m1), Sglt1(*Slc5a1*, Mm00451203_m1) and RN18S (Mm03928990_g1).

Immunoblotting analysis. Approximately 40 mg of upper or lower upper intestine were processed to yield total protein lysates, which were quantified using a BCA protein assay kit (Thermo Fisher Scientific). Twenty-five mg of protein were mixed with Laemmli buffer and loaded into 12% polyacrylamide gels. Samples were resolved by electrophoresis using a mini-Protean system (Bio-Rad) and transferred to polyvinylidene fluoride (PVDF) membranes, which were immunoblotted with antibodies for non-phospho (active) β-catenin Ser33/37/Thr41 (D13A1) (Cell Signaling, 1:1000, cat# 8814), phosphorylated (inactive) β-catenin (D10A8) (Cell Signaling, 1:1000, cat#

8480) and β-actin (13E5) (Cell Signaling, 1:1000, cat# 4970) as a loading control. Membranes were thereafter incubated with HRP-linked anti-rabbit secondary antibody (Cell Signaling, 1:10000, cat# 7074). Image documentation was carried out after incubation with Clarity Western ECL Substrate (Bio-Rad) in a ChemiDoc Imager (Bio-Rad).

Metabolic phenotyping. All tests in mice were conducted after at least 7 weeks of continuous microbial colonization via oral gavage. A glucose tolerance test (GTT, 4 g glucose/kg oral or 2 g glucose/kg *i.p.*) or insulin tolerance test (ITT, 0.8 UI/kg, *i.p.*) was done after 6 h of fasting (from 8:00 to 14:00). For pharmacological inhibition of Sglt1 in mice, GTT was performed 1h after *i.p.* injection with phloridzin (P3449, Sigma-Aldrich, 0.04 g/kg) or (vehicle 10% DMSO and 10% ethanol in 0.9% saline). A glucose-stimulated insulin secretion test (GSIS, 4 g glucose/kg oral) was done after 12 h of fasting (from 21:00 to 9:00). Blood glucose measurements were taken by tail blood. Insulin and c-peptide were assessed using a mouse insulin/c-peptide multiplex ELISA kit (Millipore, Cat. #MMHMAG-44K). Body fat composition was measured using whole body MRI (Bruker Minispec LF90-II).

*Bacterial profiling***.** Isolation of DNA from fæcal pellets was done using mechanical and enzymatic lysis. The V3-4 region of the 16S rRNA gene was PCR amplified with barcode tags compatible with Illumina technologies and the Illumina MiSeq platform was used to sequence amplified DNA products. Briefly, 50 ng of DNA was used as template with 1U of Taq, 1x buffer, 1.5 mM MgCl2, 0.4 mg/mL BSA, 0.2 mM dNTPs, and 5 pmoles each of 341F (CCTACGGGNGGCWGCAG) and 806R (GGACTACNVGGGTWTCTAAT) Illumina adapted primers. The reaction was carried out at 94 ºC for 5 minutes, 5 cycles of 94 C for 30 seconds, 47C for 30 seconds and 72C for 40 seconds, followed by 25 cycles of 94 ºC for 30 seconds, 50 ºC for 30 seconds and 72 ºC for 40 seconds, with a final extension of 72 ºC for 10 minutes. Resulting PCR products were visualized on a 1.5%

agarose gel. Details are available at www.surettelab.ca/protocols. A custom pipeline was used to process the FASTQ files. DADA2 [1] was used to assign reads to Amplicon Sequence Variants (ASVs) and assign taxonomy with the Ribosomal Database Project (RDP) Bayesian classifier using the Silva 132 database [2]. ASVs were clustered at 99% identity. Custom R scripts were used to calculate taxonomic relative abundance values, α- and β-diversity, and to perform statistical tests. In heat maps, relative abundance of each taxon was expressed as $\log_{10}$ fold change from its median across the entire cohort. All relative abundance values of 0 were assigned 1×10^{-6} in heat maps, one order of magnitude lower than the lowest detectable taxon in the dataset, to allow the logarithmic transformation of the fold change.

Supplemental figures:

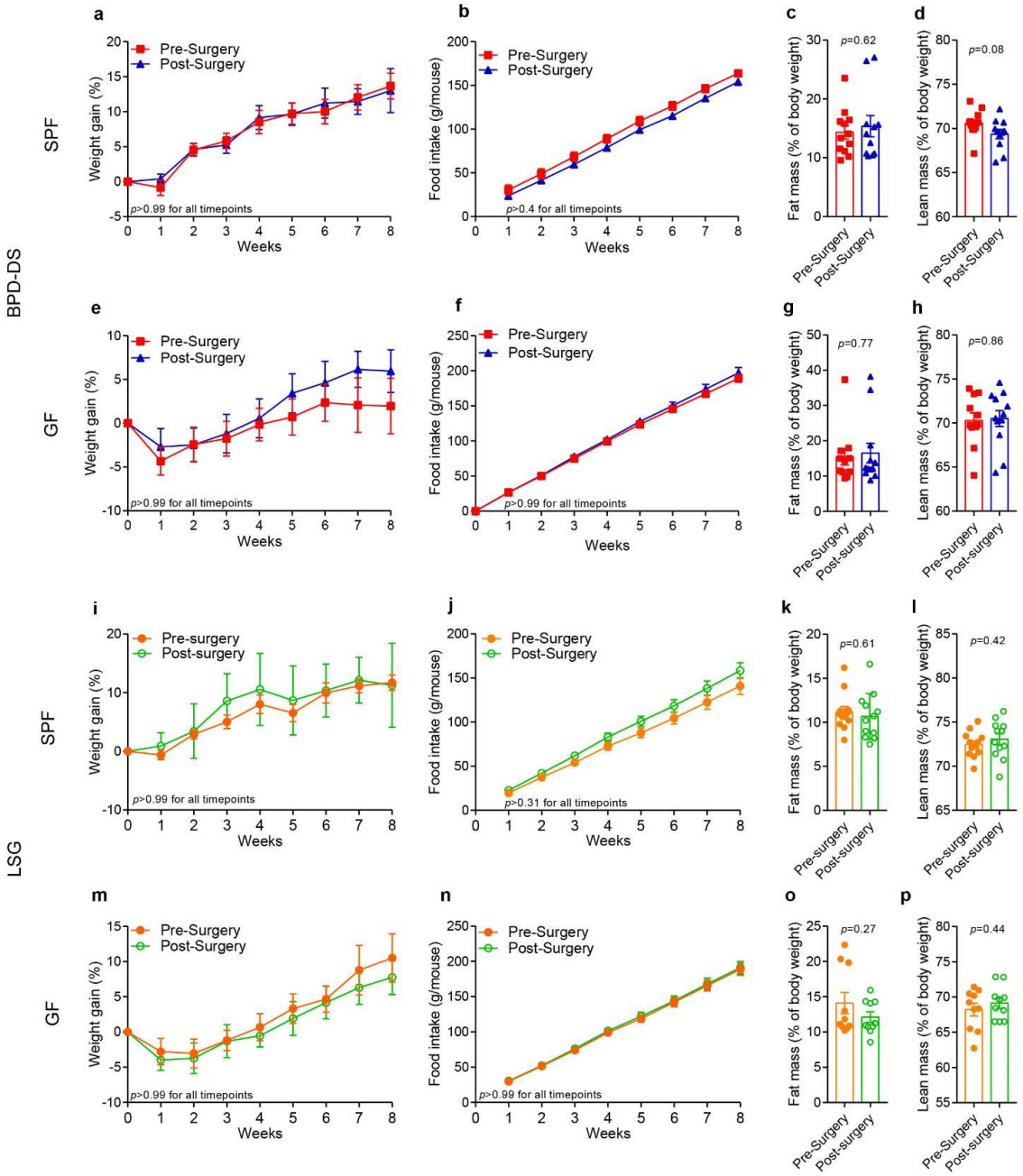
BPD-DS
LSG
SPF
GF
a
b
c
d
e
f
g
h
i
j
k
l
m
n
o
p
Pre-Surgery
Post-Surgery
Pre-surgery
Post-surgery
Weight gain (%)
Food intake (g/mouse)
Fat mass (% of body weight)
Lean mass (% of body weight)
Weeks
p>0.99 for all timepoints
p>0.4 for all timepoints
p>0.31 for all timepoints
p=0.62
p=0.08
p=0.77
p=0.86
p=0.61
p=0.42
p=0.27
p=0.44

Supplemental figure 1: Body features in mice colonised with the fæcal microbiota of patients before and after BPD-DS or LSG. (a, e) Weight gain, **(b, f)** food intake, and **(c, d, g, h)** body composition in specific pathogen-free (SPF) and germ-free (GF) female mice colonised with fæcal slurries from women before and after Biliopancreatic Diversion with Duodenal Switch. **(i, m)** Weight gain**, (j, n)** food intake, and **(k, l, o, p)** body composition in SPF and GF female mice colonised with fæcal slurries from women before and after Laparoscopic Sleeve Gastrectomy (LSG). Data are presented as the mean ±SEM. Unpaired student's t-test was used to assign statistical significance to pairwise comparisons. For repeated measurements throughout time, repeated measures two-way ANOVA followed by pairwise comparisons with a Tukey post-test were performed. Statistical significance was accepted at $p<0.05$. Each square, triangle and circle represents a biological replicate (n=11-12).

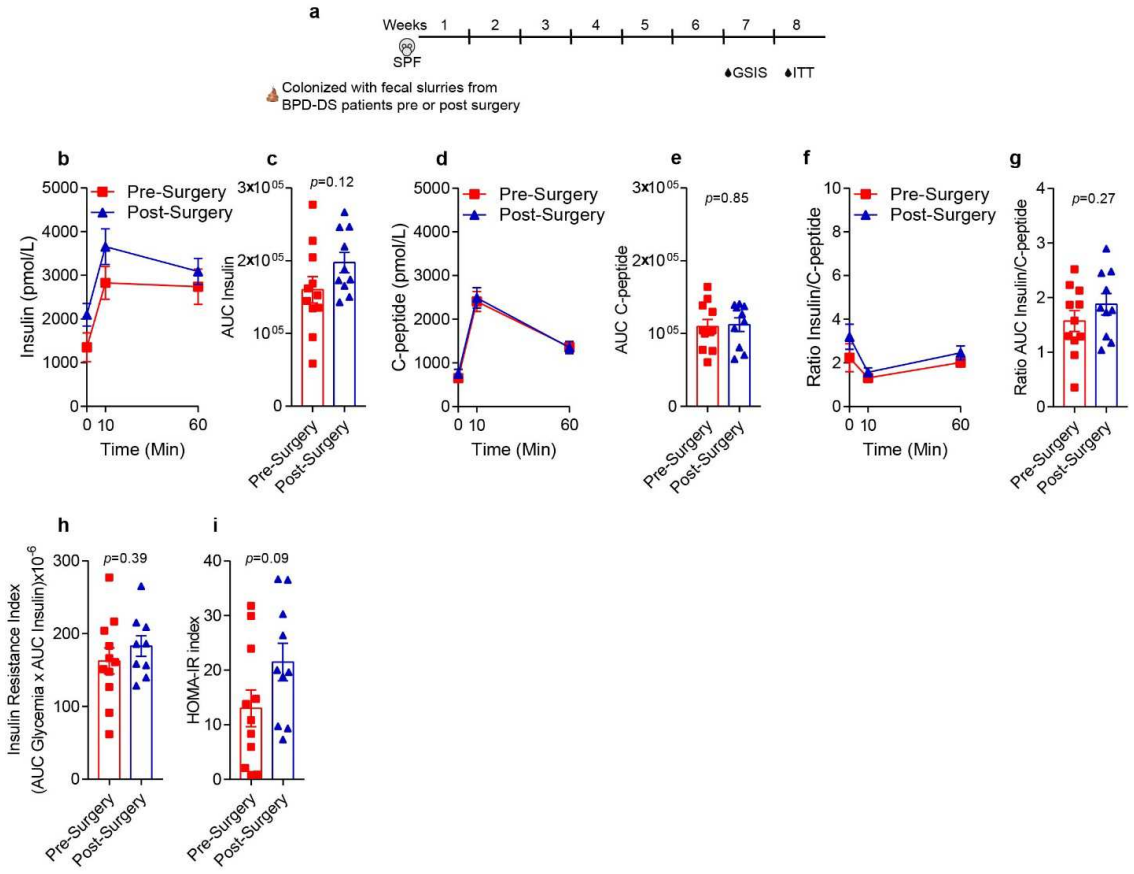

Supplemental Figure 2: Glucose-stimulated insulin and c-peptide levels in mice colonised with the fæcal microbiota of patients before and after BPD-DS. (a) Timeline of metabolic profiling in specific pathogen-free (SPF) female mice colonised with fæcal slurries from women before and after Biliopancreatic Diversion with Duodenal Switch (BPD-DS). **(b, c)** Plasma insulin, **(d, e)** c-peptide, and **(f, g)** insulin/c-peptide ratio during glucose-stimulated insulin secretion (GSIS) tests and area under the curves (AUC). **(h)** Insulin resistance index. **(i)** HOMA-IR. Unpaired student's t-test was used to calculate *p* values, which were considered significant at $p<0.05$. Each square and triangle represents a biological replicate (n=10-12).

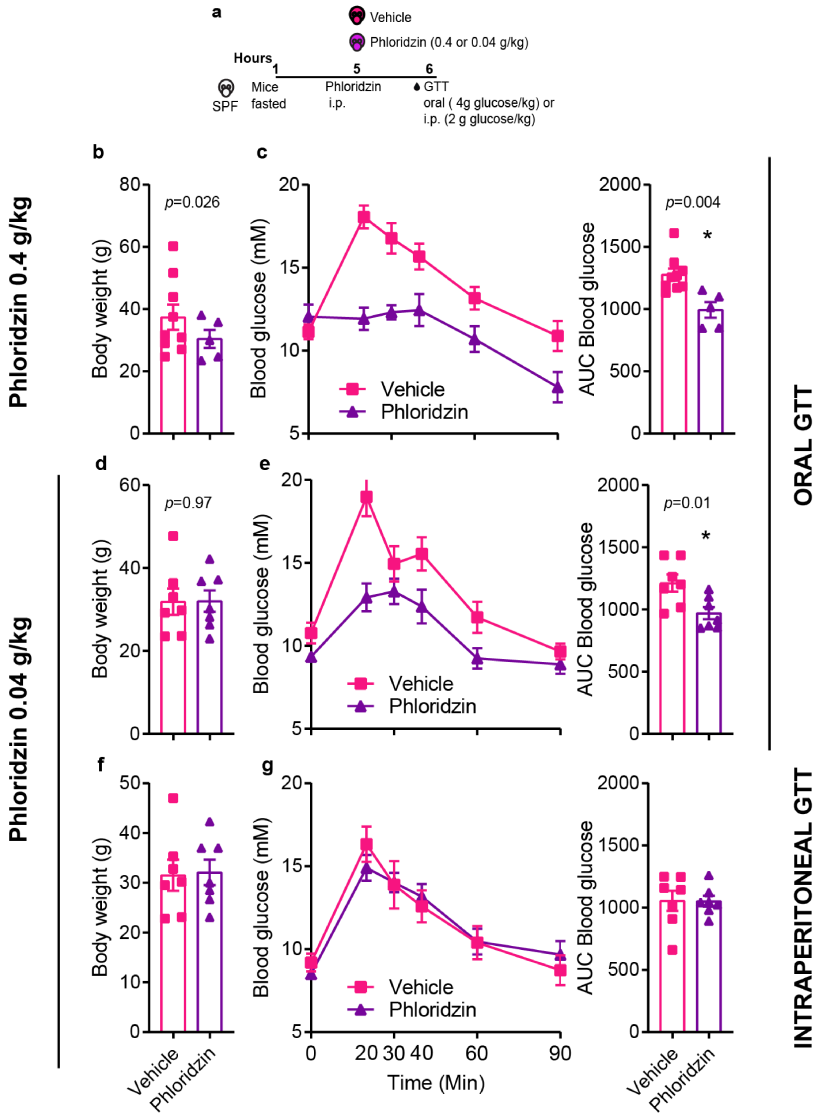

Supplemental figure 3: A low dose of phloridzin attenuates blood glucose upon oral, but not intraperitoneal, GTT in mice. (a) Female specific pathogen-free (SPF) mice were intraperitoneally injected with 0.4 or 0.04 g/kg phloridzin or vehicle and next subjected to oral or intraperitoneal glucose tolerance tests (GTT). Body weight, glucose excursion during oral GTT and area under GTT curves (AUC) after injection with **(b, c)** 0.4 g/kg and **(d, e)** 0.04 g/kg phloridzin. **(f, g)** Body weight, glucose excursion during intraperitoneal GTT and AUC after injection with 0.04 g/kg. Data are presented as the mean ±SEM. Unpaired student's t-test was used to calculate *p* values, which were considered significant at $p<0.05$. Each square or triangle represents a biological replicate (n=5-9)

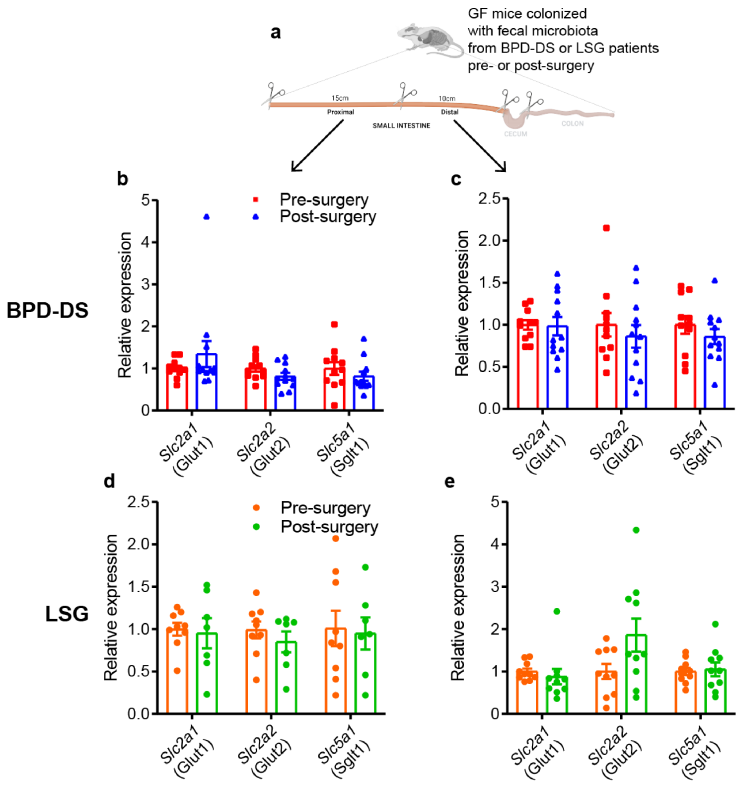

Supplemental figure 4: Transcript levels of glucose transporters in the gut of mice colonised with the fæcal microbiota of patients before and after BPD-DS or LSG. (a) mRNA was purified from proximal and distal small intestine sections from female germ-free (GF) mice colonised with fæcal microbiota of women before and after Bioliopancreatic Diversion with Duodenal Switch (BPD-DS) or Laparoscopic Sleeve Gastrectomy, reverse transcribed and used for RT-qPCR analysis. The mRNA expression of genes encoding Glut1 (*Slc2a1*), Glut2 (*Slc2a2*) and Sglt1 (*Slc5a1*) were analyzed using the ΔΔCt method and 18S as reference gene in the proximal and distal intestine of mice colonised with the fæcal microbiota before and after **(b, c)** BPD-DS or **(d, e)**. Data are presented as the mean ±SEM. Unpaired student's t-test was used to calculate *p* values, which were considered significant at $p<0.05$. Each square, triangle or circle represents a biological replicate (n=7-11)

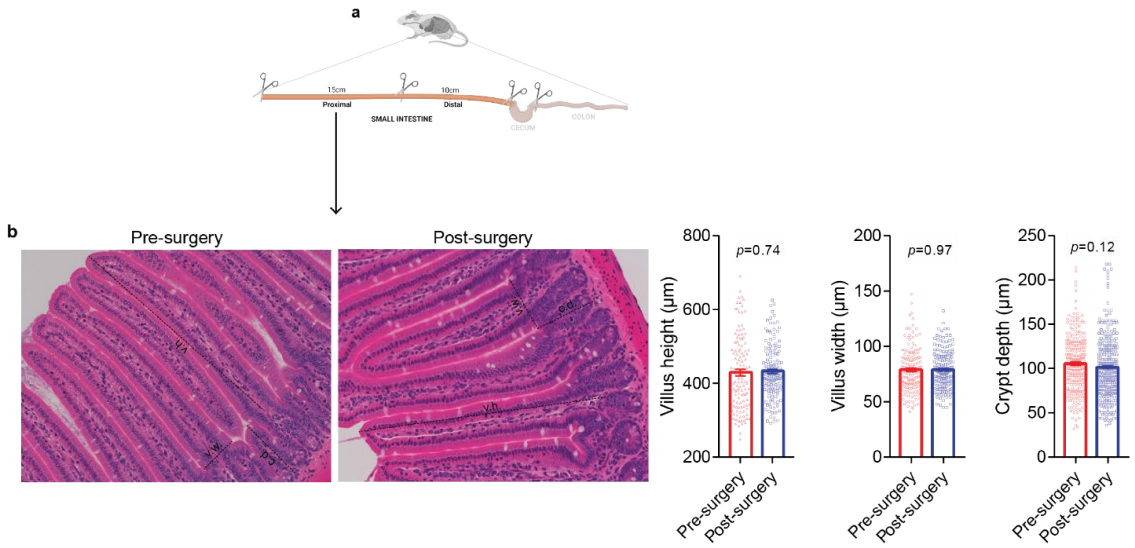

Supplemental figure 5: Intestinal morphology in the proximal small intestine of mice colonised with the fæcal microbiota of patients before and after BPD-DS. (a) Schematic representation of method used to separate and harvest different intestinal sections from mice. **(b)** Representative images and morphometric analysis of hematoxylin/eosin-stained proximal small intestine sections harvested from female germ-free (GF) mice colonised with the fæcal microbiota of female patients before and after Bioliopancreatic Diversion with Duodenal Switch (BPD-DS). Each dot represents a villus or crypt (ie, technical replicates, n=122-296).

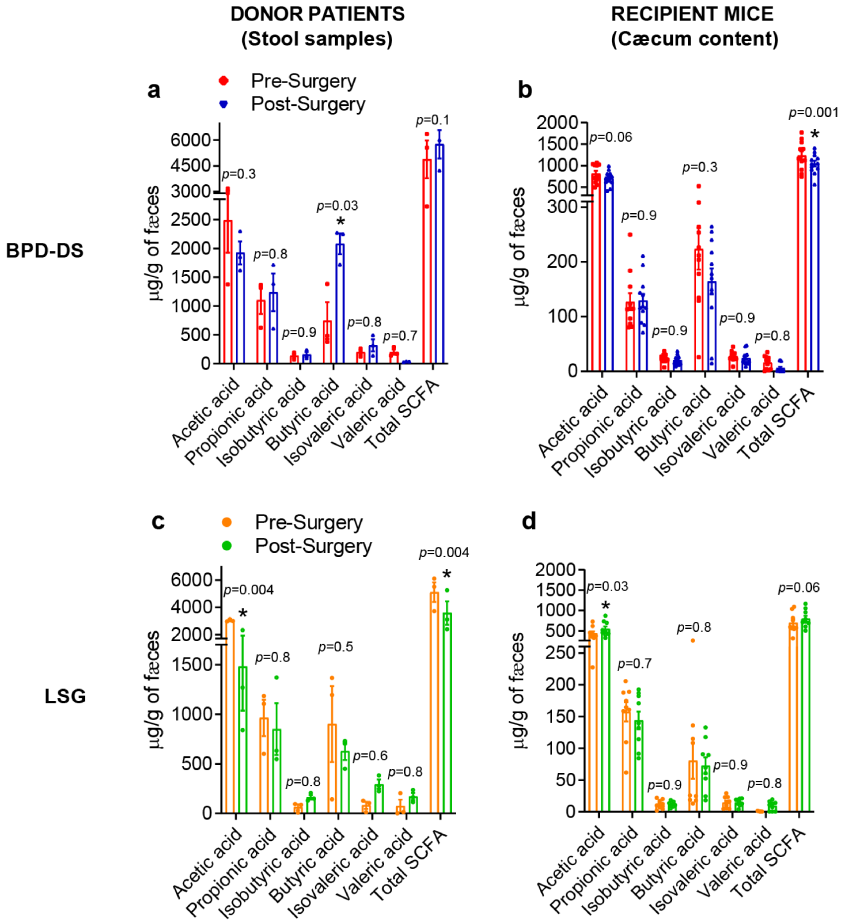

Supplemental figure 6: Short-chain fatty acids in patients and recipient mice before and after BPD-DS or LSG. (a, c) Short-chain fatty acids (SCFAs) found in stool samples from women before and after Biliopancreatic Diversion with Duodenal Switch (BPD-DS) or Laparoscopic Sleeve Gastrectomy (LSG) (n=3). **(b, d)** SCFAs in the cæcum of female mice colonised with fæcal slurries from women before and after BPD-DS or LSG (n= 11-12). Data are presented as the mean ±SEM. Unpaired student's t-test was used to calculate *p* values, which were considered significant at $p<0.05$. Each square or triangle or circle represents a biological replicate.

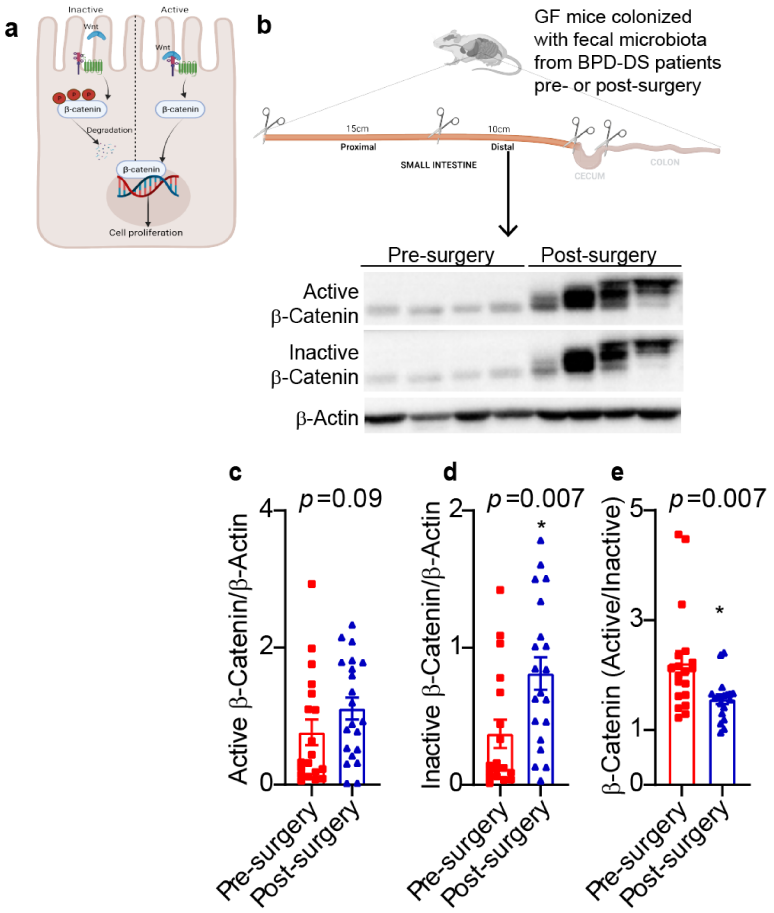

Supplemental Figure 7: Protein expression of active and inactive β-catenin in the gut of mice colonised with the fæcal microbiota of patients before and after BPD-DS (a) Upon phosphorylation, β-catenin is primed to proteasomal degradation and remains inactive. Receptor activation by a wnt ligand instigates downstream signals to dephosphorylate and activate β-catenin, which in turn regulates cell proliferation. **(b)** Protein lysates were obtained from distal small intestine sections from female germ-free (GF) mice colonised with fæcal microbiota of women before and after Bioliopancreatic Diversion with Duodenal Switch (BPD-DS) and immunoblotted against active and inactive β-catenin as well as β-actin as a loading control. Membrane picture is representative of the entire cohort and one band was cropped out of the image on each side. Bands were analyzed by densitometry, and protein expression of **(c)** active and **(d)** inactive β-catenin was normalized by the loading control. **(d)** The ratio Active:Inactive β-catenin was calculated as a readout of Wnt/ β-catenin pathway activation status. Data are presented as the mean ±SEM. Unpaired student's t-test was used to calculate *p* values, which were considered significant at $p<0.05$. Each square or triangle represents a biological replicate (n=17-21)

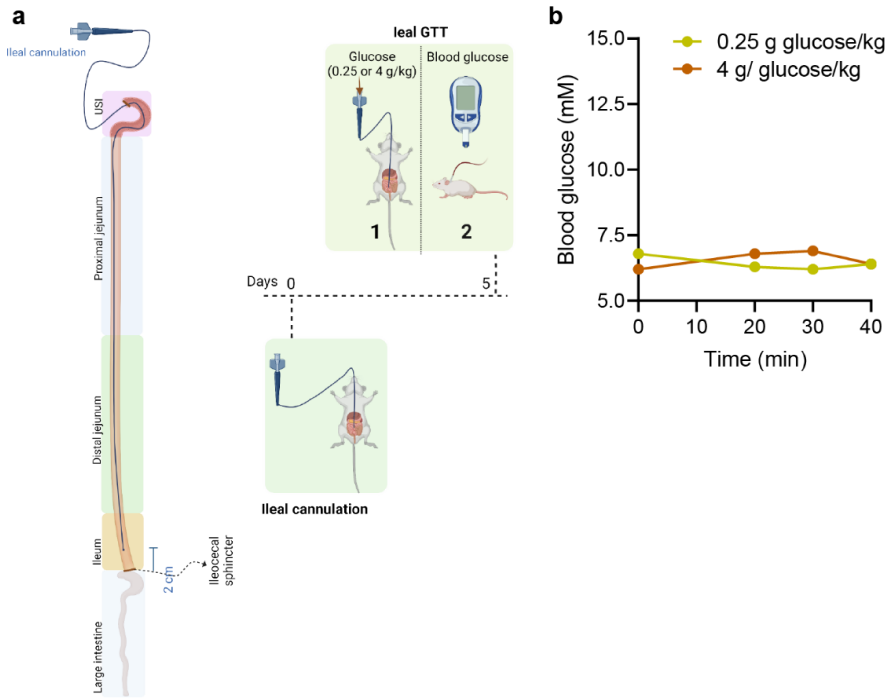

Supplemental Figure 8: Blood glucose after intraluminal glucose infusion in the ileum of rats. **(a)** A catheter was placed into the ileum (2 cm distal to the ileocecal valve) of specific pathogen-free (SPF) male rats. One day after ileal cannulation, rats were infused with 0.25 or 4 g/kg glucose targeting the distal ileum and large intestine. Blood glucose was monitored at different time points (0, 5, 10, 20, 30, 40 min) after glucose infusion. **(b)** Glucose excursion curves following glucose infusion into the ileum and large intestine (n=1).

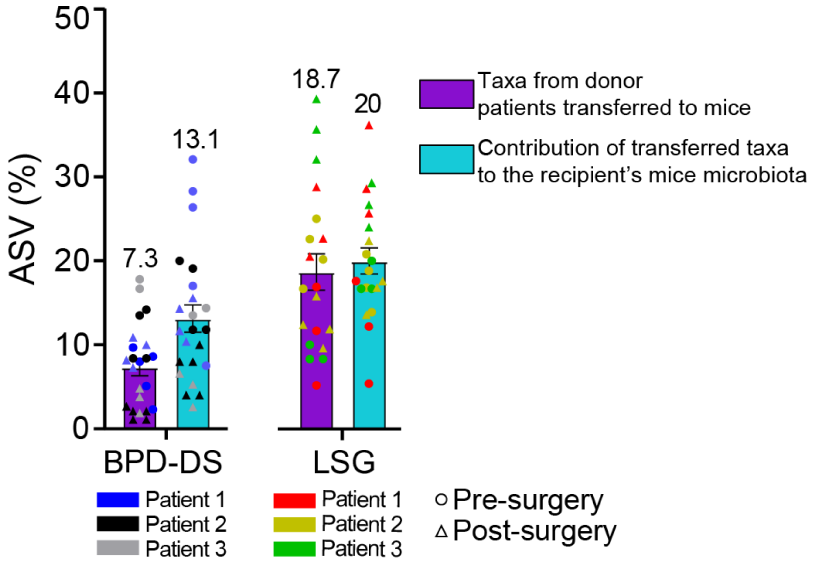

Supplemental Figure 9: Colonisation efficiency in mice colonised with the fæcal microbiota of patients before and after BPD-DS or LSG. The purple columns show the percentage of ASVs found in the inocula (fæces from donor patients) and that were also identified in the fæces of recipient mice (ie, transmitted taxa). The ocean blue columns show the percentage contribution of transmitted taxa to the recipient mice's microbiota. Each circle or triangle represents a mouse (independent biological replicates), where the shape indicates pre- or post-surgery timepoint and the colour indicates the origin of the inoculum. Data are presented as the mean ±SEM

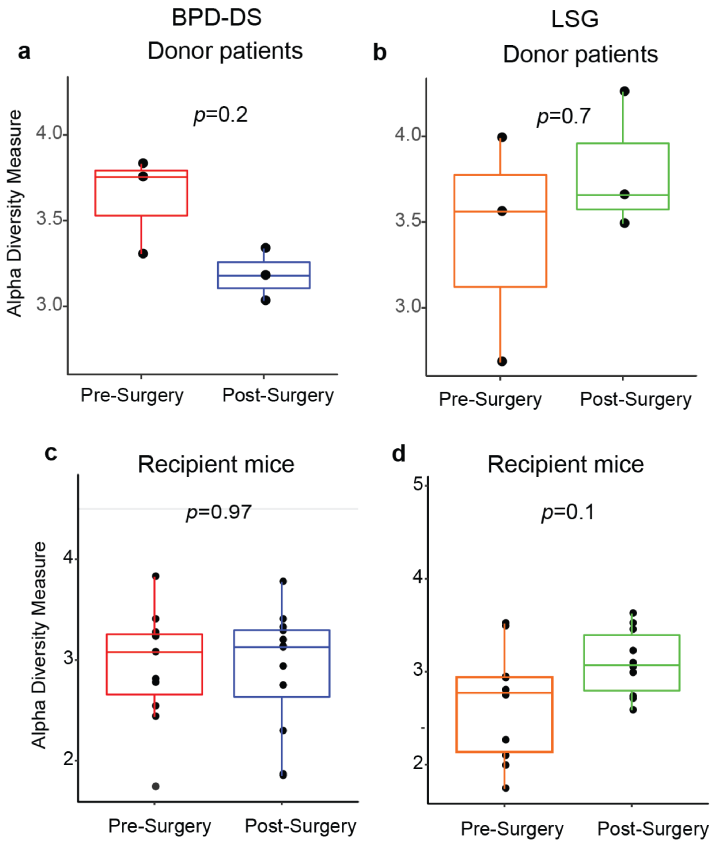

Supplemental Figure 10: Alpha-diversity in stool samples of mice colonised with the fæcal microbiota of patients before and after BPD-DS or LSG. Taxonomically annotated 16S rRNA gene sequences were quantified and used to calculate the Shannon Index to infer within-sample diversity. Shannon index was calculated with taxa obtained from stool samples of women before and after **(a)** BPD-DS and **(b)** LSG (n=3). Shannon index was also calculated for fæcal bacterial communities found in the in female germ-free (GF) mice colonised with fæcal microbiota from women before and after **(a)** BPD-DS or **(b)** LSG (n=10-12). Unpaired student's t-test was used to calculate *p* values, which were considered significant at $p<0.05$. Each dot represents a biological replicate (n=10-12).

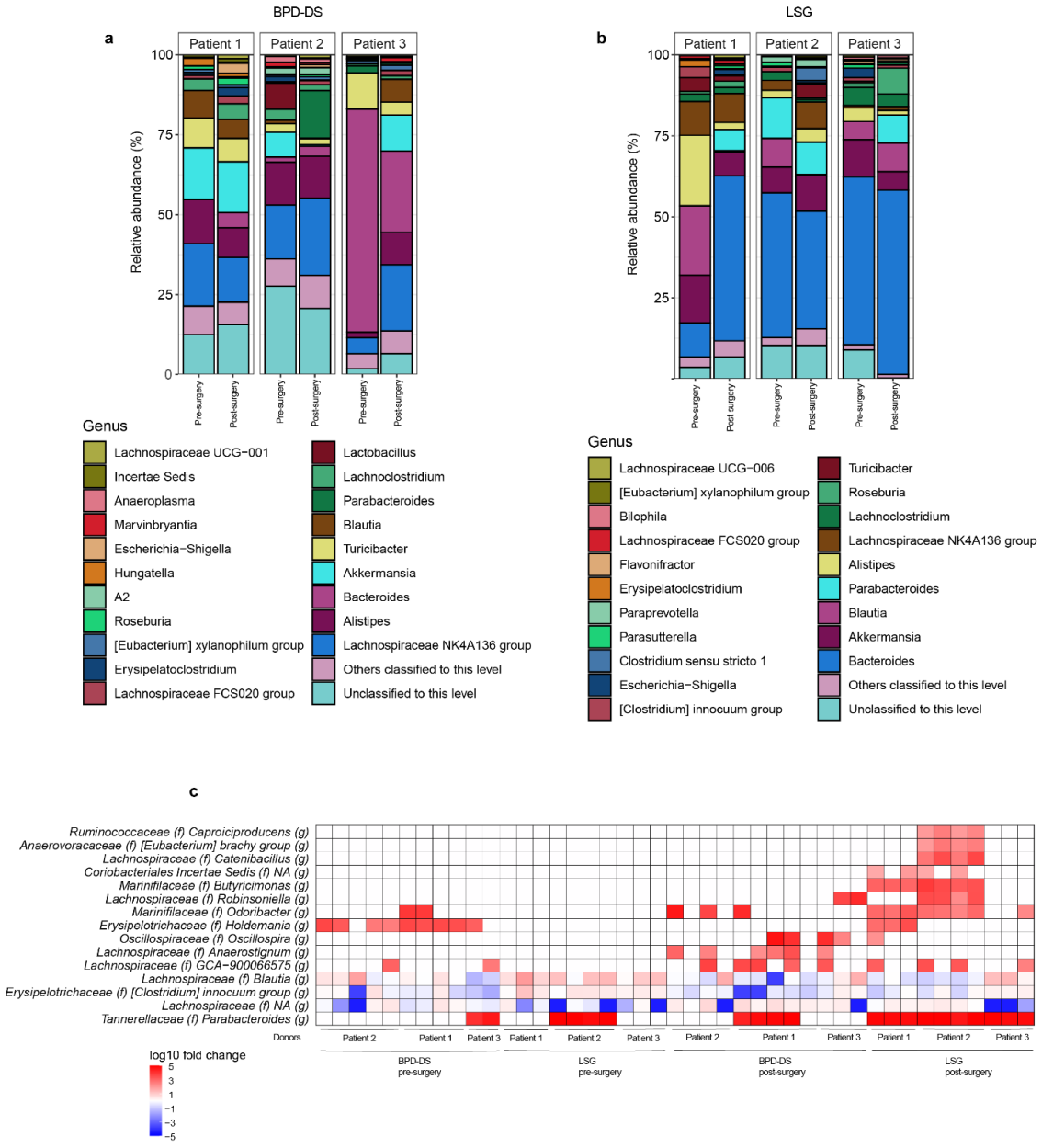

Supplemental figure 11: Bacterial relative abundance profile in the fæces of mice colonised with the fæcal microbiota of patients before and after BPD-DS or LSG. Relative abundance of the top 20 most abundant bacterial genera in the fæces of female germ-free (GF) recipient mice colonised with the fæcal microbiota of women before and after **(a)** Bioliopancreatic Diversion with Duodenal Switch (BPD-DS) or **(b)** Laparoscopic Sleeve Gastrectomy (LSG). **(c)** Heat maps depicting the taxa significantly different between the pre- and post- surgery groups (p<0.05,

Wilcoxon rank sum test). ASVs were clustered at 99% similarity and grouped by genus. The relative abundance of each taxon is expressed as $\log_{10}$ fold change from its median level across the entire cohort (both surgeries combined). All relative abundance values of 0 were assigned 1×10^{-6}, one order of magnitude lower than the lowest detectable taxon in the dataset, to allow the logarithmic transformation of the fold change. The heat map is clustered along both axes. Each square, triangle and circle represent a biological replicate n=11-12.

Supplemental tables:

Supplemental Table 1: Medicaments used by donor patients

Donor	Surgery type	Medicaments pre-surgery	Medicaments post-surgery
1	BPD-DS	Metformin 500 mg, Levothyroxine 0.2 mg, Formoterol, Budesonide, Fluconazole 150 mg	
2	BPD-DS	Metformin 850 mg, Insulin isophene 100 U, Insulin lispro 5-10 U of TDI, Pantoprazole 40 mg	Pancrelipase 10000 IU
3	BPD-DS	Metformin 500 mg, Rosuvastatin 5 mg, Acetaminophen 650 mg	
1	LSG	Ranitidine 150 mg, Hydrocodone-Phenylephrine syrup, Levonogestrel IUD (20 µg/day), Acetaminophen 500 mg, Acyclovir topical cream	Acetaminophen 500 mg, Velacyclovir 500 mg
2	LSG	Metformin 850 mg, Canagliflozin 300 mg, Rosuvastatin 5 mg, Morphine 5 mg, Acetaminophen 325 mg	Acetaminophen 650 mg Buprenorphine skin patch 1µg/h.
3	LSG	Rabeprazole 20 mg	Lansoprazole 30 mg Estradiol 0.06% topical cream

Note: Data post-surgery was obtained 12 months after bariatric procedure. TDI stands for Total Daily Insulin. IUD stands for Intrauterine Device. BPD-DS and LSG are acronyms for Biliopancreatic Diversion with Duodenal Switch and Vertical Sleeve Gastrectomy, respectively.

Supplemental Table 2: Caloric intake by donor patients

			Patient 1	Patient 2	Patient 3
BPD-DS	Pre-surgery	Energy (kcal)	3072.5	1992.4	2818.6
		% calories from fat	39.7	28.9	44.4
		% calories from protein	17.4	19.6	15.9
		% calories from carbohydrate	41.9	52.9	42.9
	Post-surgery	Energy (kcal)	2793.2	1836.2	2295.5
		% calories from fat	39.6	29.2	43.7
		% calories from protein	17.0	18.8	14.4
		% calories from carbohydrate	41.7	52.8	44.8
		Caloric restriction (kcal)	279.2	156.2	523.0
		Caloric restriction (%)	9.1	7.8	18.6
LSG	Pre-surgery	Energy (kcal)	1873.6	1800.0	3432.7521
		% calories from fat	35.4	38.3	32.2342
		% calories from protein	18.9	24.3	21.3723
		% calories from carbohydrate	47.3	38.9	48.72
	Post-surgery	Energy (kcal)	2402.8	1115.0	not available
		% calories from fat	41.7	42.7	
		% calories from protein	20.3	18.8	
		% calories from carbohydrate	41.0	40.0	
		Caloric restriction (kcal)	-529.2	685.0	
		Caloric restriction (%)	128.2	61.9	

Note: Data post-surgery was obtained 12 months after bariatric procedure. BPD-DS and LSG are acronyms for Biliopancreatic Diversion with Duodenal Switch and Vertical Sleeve Gastrectomy, respectively.

References:

1 Callahan BJ, McMurdie PJ, Rosen MJ, *et al.* DADA2: high-resolution sample inference from Illumina amplicon data. *Nat Methods* 2016;**13**:581–3.

2 Quast C, Pruesse E, Yilmaz P, *et al.* The SILVA ribosomal RNA gene database project: improved data processing and web-based tools. *Nucleic Acids Res* 2012;**41**:D590–6.